Check for updates

European Journal of Soil Science

WILEY

European Journal of Soil Science

RESEARCH ARTICLE OPEN ACCESS

Placement of Acidified Biowastes: Unveiling Abiotic and Biotic Effects on Soil P Dynamics Using ^{18}O as a Tracer

Pietro Sica[1,2] | Maria Monrad Rieckmann[1] | Mario Álvarez Salas[1,3] | Jakob Magid[1] | Federica Tamburini[3]

[1]Department of Plant and Environmental Sciences, University of Copenhagen, Frederiksberg, Denmark | [2]Department of Food Science and Technology, College of Agriculture Luiz de Queiroz, University of São Paulo, São Paulo, Brazil | [3]Group of Plant Nutrition, Institute of Agricultural Sciences, ETH Zurich, Lindau, Switzerland

Correspondence: Pietro Sica (pietro@plen.ku.dk; pietro.sica@usp.br) | Jakob Magid (jma@plen.ku.dk)

Received: 11 March 2024 | **Revised:** 21 January 2025 | **Accepted:** 3 February 2025

Funding: This project has received funding from the European Union's Horizon 2020 research and innovation programme under the Marie Sklodowska-Curie grant agreement No. 860127 and from the Independent Research Fund Denmark, under the project PROCESSOR (Phosphorus Recycling frOm Complex scarcEly Soluble Societal resources – letting the sOil do the work), grant number 1032-00011B.

Keywords: biogeochemical processes | digestate solid fraction | meat and bone meal | P availability | P diffusion | P incubation study | P release mechanisms

ABSTRACT

Placement and acidification can improve phosphorus (P) availability from biowastes. However, little is known about how the placement of acidified biowastes affects biotic and abiotic processes in the soil. Thus, we selected two biowastes: digestate solid fraction (DSF) and meat and bone meal (MBM). Both were applied in their untreated and acidified forms. We hypothesised that the acidification would affect biotic and abiotic processes and, consequently, the P dynamics in the soil. All fertilisers were incubated for 12 days to evaluate abiotic and biotic processes in the placement zone and in the adjacent soil. Assessments included resin-extractable P (resin P) and microbial P contents and $\delta^{18}O$ values at different distances from the placement zone. Microbial respiration was also measured. Acidification significantly increased P release for DSF and MBM. The soil resin P content of acidified biowastes was larger even at greater distances (10–12 mm). For untreated MBM, soil resin P was significantly larger than the negative control up to 4 mm from the placement zone (50–60 mg kg^{-1}). For this treatment, microbial P was relatively increased even at greater distances (150 mg kg^{-1} at 6–8 mm). Acidification suppressed microbial activity and resulted in lower respiration rates for both MBM and DSF. In addition to that, our results showed a significant correlation between ^{18}O incorporation into microbial P and microbial respiration. Thus, the greater the microbial activity, the more P is biologically cycled in the microbial biomass. However, no correlation was found between respiration and ^{18}O incorporation into resin P. These results may indicate an insufficient incubation time for microbes to release P into the soil and/or the co-occurrence of abiotic processes which are not exchanging oxygen between water and phosphate (e.g., desorption). We conclude that for untreated MBM, biotic processes may be the main driver of P movement in the soil. In the case of acidified biowaste, diffusion is the main process moving the P in the soil. This research shows that acidifying biowastes like DSF and MBM boosts P availability through abiotic processes. These findings suggest that acidification can enhance nutrient use efficiency and improve soil fertility. However, further studies are needed to assess the long-term effects on microbial communities and soil health.

1 | Introduction

Mineral phosphorus (P) fertiliser prices have fluctuated considerably in recent years (Baffes and Koh 2022; Ibendahl 2022). On the one hand, the European Union is highly dependent on the imports of these materials. On the other hand, large amounts of P-biowastes are generated in this region (Salas et al. 2024). Efficient recycling of P from organic materials—such as animal

This is an open access article under the terms of the Creative Commons Attribution-NonCommercial-NoDerivs License, which permits use and distribution in any medium, provided the original work is properly cited, the use is non-commercial and no modifications or adaptations are made.

© 2025 The Author(s). *European Journal of Soil Science* published by John Wiley & Sons Ltd on behalf of British Society of Soil Science.

Summary

- Acidification inhibited microbial activity and affected C, N, and P dynamics in the soil.
- Acidification increased P released from the fertiliser and diffusion through the soil.
- For untreated meat and bone meal, microbial growth transported P through the soil.
- ^{18}O incorporation into the microbial P was significantly correlated with microbial respiration.

manures, meat and bone meal, and sewage sludge—has the potential to meet most of the European Union's annual P demand, estimated at approximately 3300 Gg P (van Dijk et al. 2016). These organic sources and animal-derived biowastes could collectively contribute up to 2950 Gg P per year. Therefore, animal-derived biowastes, such as meat and bone meal and digestates, may be able to replace mineral P fertilisers in agriculture and reduce the European Union's dependence on mineral P fertiliser imports (Recena et al. 2022).

Meat and bone meal is a biowaste composed of dried and ground bones, blood, and residual meats from slaughterhouses (Christiansen et al. 2020). It has large carbon (C) (~40%) and nitrogen (N) (~10%) contents, which are mainly derived from organic compounds in the meat and blood (Kivelä et al. 2015), while its P is mainly derived from the bones (Jeng et al. 2007) in the form of hydroxyapatite (Hernandez-Mora et al. 2024).

Another example of a relevant animal-derived biowaste is the digestate solid fraction. The solid–liquid separation of animal slurry, manure, and digestate is a simple technology that facilitates the recovery of most N and dissolved organic matter in the liquid fraction, while P and more stable forms of organic matter remain in the solid fraction (Tambone et al. 2017; Chuda et al. 2021). As a result, this approach allows for more efficient management of digestate nutrients, as the solid fraction contains high P content, mainly formed by Ca- and Mg-bound P and struvite precipitated in the anaerobic digestion reactor (Möller and Müller 2012; Bruun et al. 2017).

In both meat and bone meal and the solid fraction of digestate, P is poorly soluble in water (Christiansen et al. 2020; Regueiro et al. 2020; Sica, Kopp, Müller-Stöver, et al. 2023). Consequently, both biowastes have a lesser P fertiliser value compared to mineral fertilisers. As an alternative to increasing their P fertiliser value, Sica, Kopp, Müller-Stöver, et al. (2023) identified acidification with sulphuric acid among different treatments as the most promising method for increasing the P solubility and availability of meat and bone meal and digestate solid fraction when placed in the soil (Sica, Kopp, Müller-Stöver, et al. 2023; Sica, Kopp, Magid, et al. 2023; Sica and Magid 2024). Thus, the acidification of biowastes may be an approach to increase their fertiliser value and formulate P-efficient biobased fertilisers.

However, little is known regarding the effects of acidification on physical, chemical, and biological interactions between the soil and the applied fertiliser within the placement zone and its adjacent soil. Studies to elucidate these interactions are essential to uncover the mechanisms responsible for affecting P availability to crops and assess the potential effects on plant growth (Meyer et al. 2020, 2021, 2023; Sica, Kopp, Müller-Stöver, et al. 2023). The placement of biowastes will create a nutrient-rich patch in the placement zone that may expand through the soil, releasing N, P, and C, which may favour microbial growth and intensify chemical and physical processes in this "hot-spot" (Pedersen et al. 2020; Baral et al. 2021; Sica, Kopp, Müller-Stöver, et al. 2023). Thus, while diffusion is the primary driver of abiotic P transport in soils, P immobilisation and microbial growth can also affect transport through the soil via fungal highways (Ruess and Ferris 2004).

For instance, Sica, Kopp, Müller-Stöver, et al. (2023) observed a considerable microbial growth in the placement zone and surrounding soil of meat and bone meal. The authors suggested that microbes grow from the placement zone, taking up nutrients from the meat and bone meal, including P, and transporting them through the soil. However, it is difficult to (i) distinguish the effects of physical processes (diffusion) from biological processes on the transport of P from the placement zone through the soil, and (ii) determine whether the P is transported away from the fertiliser by the movement of the microbes or whether there is a sequence of processes: uptake, intracellular cycling, release, diffusion, cycle starts again. For that, analyses of microbial P at different distances from the fertiliser placement zone (fertiliser layer) and the determination of the oxygen isotope composition of soil resin and microbial P pools ($\delta^{18}O$-P) after labelling the soil solution with ^{18}O-enriched water are tools to assess biotic P turnover in soil (Tamburini et al. 2012).

The $\delta^{18}O$-P value refers to the ratio of stable oxygen isotopes (^{16}O and ^{18}O), in phosphate (PO_4^{3-}) in a sample, compared to the Vienna Standard Mean Ocean Water (VSMOW) standard (Blake et al. 2005). The $\delta^{18}O$-P value undergoes changes due to biological processes incorporating oxygen from water, while negligible fractionation occurs due to abiotic processes (e.g., sorption and desorption from solid particles) at ambient temperatures compared to biotic processes (Blake et al. 2005). In the placement zone of fertilisers in soils, two main effects related to microbial P cycling are expected to occur: (i) The pyrophosphatase-driven isotopic equilibrium between oxygen in water and phosphate. In soils, $\delta^{18}O$-P values are typically found in equilibrium with soil water. This equilibrium is driven by the intracellular enzyme pyrophosphatase. This enzyme catalyses the hydrolysis of pyrophosphates, commonly formed during cell metabolic processes, into two separate phosphates, requiring the acquisition of an oxygen atom from the surrounding water. As this process is rapid and continuous, it eventually exchanges all oxygen atoms in the phosphate with those from the surrounding water, resulting in isotopic equilibrium (Chang and Blake 2015). (ii) The release of ^{18}O-depleted phosphate deriving from the activity of extracellular phosphatase as a strategy to solubilise and acquire inorganic phosphate (von Sperber et al. 2014). Oxygen isotopes can be used to trace both processes, making them a valuable tool for discerning the role of microorganisms in soil P cycling (Frossard et al. 2011; Tamburini et al. 2012; Pistocchi et al. 2020; Siegenthaler et al. 2020).

Based on this background, this study aimed to elucidate the effects of both biotic and abiotic processes on P dynamics within

13652389, 2025, 2, Downloaded from https://bsssjournals.onlinelibrary.wiley.com/doi/10.1111/ejss.70076 by Capes, Wiley Online Library on [17/03/2025]. See the Terms and Conditions (https://onlinelibrary.wiley.com/terms-and-conditions) on Wiley Online Library for rules of use; OA articles are governed by the applicable Creative Commons License

the placement zone and surrounding soil of untreated and acidified biowastes. We hypothesised that:

1. Fertliser composition and acidification pre-treatment will affect biotic and abiotic processes in the placement zone and surrounding soil.
2. For untreated biowastes, P movement from the placement zone through the soil is primarily driven by biotic processes (as indicated by intracellular isotopic equilibration of oxygen between water and phosphate and by released of phosphate by hydrolytic enzymes), with microbial growth serving as the principal transport mechanism.
3. The placement of acidified biowastes will increase the soluble P applied and lower the soil pH surrounding the placement zone to levels that inhibit microbial activity. As a result, the movement of P from the placement zone through the soil will be primarily driven by abiotic processes, with diffusion as the main transport mechanism.

To test these hypotheses, this study consisted of incubation experiments combining analyses such as P release from fertiliser to soil, P diffusion through abiotic processes (measured with resin-P) and biotic processes (measured with microbial-P) and pH at different distances, up to 12 mm from the placement zone, as well as microbial respiration. In addition, ^{18}O-enriched water was used to evaluate the changes in resin and microbial δ^{18}O-P values after 12 days of incubation.

Understanding the interactions between acidified biowastes and soil processes has practical implications for both agriculture and environmental management. By enhancing P availability and minimising microbial P immobilisation, this knowledge can improve nutrient use efficiency, reduce the need for synthetic fertilisers, and promote more sustainable agricultural practices. In addition, optimising the use of animal-derived biowastes as fertilisers can help to mitigate biowaste disposal issues, potentially reduce the associated environmental pollution, and promote circular resource management, contributing to more sustainable agricultural systems. However, it is worth noting that further studies may be needed to investigate the long-term effect of acidification on soil fertility, P dynamics, and soil health.

2 | Materials and Methods

2.1 | Fertilisers and Soil

In this study, two biowastes—digestate solid fraction and meat and bone meal—were selected and applied in two forms: untreated and acidified, to evaluate the effects of acidification on soil P dynamics. Hereafter, untreated and acidified biowastes are also denominated as 'fertilisers'. Triple super phosphate (hereafter 'TSP') was selected as a control mineral because it is a typical commercial mineral P fertiliser used in agriculture due to its high P content, solubility, and availability. A negative control, with no fertiliser application, was also included. This treatment was used as a reference and baseline to evaluate the effects of the treatments on the soil parameters analysed in this study.

The mineral fertiliser (TSP) was purchased in granular form, ground, and sieved (< 2 mm) before being applied in each experiment. It had 20.8% of total P, of which 80% was soluble in water. The digestate solid fraction (hereafter 'DSF') was collected from Maabjerg Energy Center, Holstebro, Denmark. This plant uses as substrate about 70% cattle manure, 20% pig slurry, 8%–9% chicken manure, and 1%–2% food waste (see Liu et al. (2019)). The meat and bone meal (hereafter 'MBM') was sourced from the Daka SecAnim plant, Hedensted, Denmark, predominantly being composed of bones and meat residues from slaughterhouses.

The total C, N, sulphur (S), and P (mg g^{-1}), the resin-P (anion exchange resin), organic P (% of the total P), and δ^{18}O-P (in the ‰ notation) of both untreated and acidified biowastes and the soil used in this study (T0) are shown in Table 1 (more details in Table S1).

Sulphuric acid and the concentration used in this study were chosen based on the results of Sica, Kopp, Magid, et al. (2023) and Sica, Kopp, Müller-Stöver, et al. (2023), who showed that these were the more efficient treatment and concentration for increasing the solubility and availability of P in MBM and DSF. Acidification of both MBM and DSF followed the procedure by Sica, Kopp, Müller-Stöver, et al. (2023) and Kopp et al. (2023). Briefly, 1.5 M sulphuric acid was homogeneously mixed with untreated MBM (one part of acid to two parts MBM by weight) and DSF (1:1 ratio by volume to weight). This application corresponds to 75 and 150 g of sulphuric acid per kg of dried material for MBM and DSF, respectively. After acid treatment, the acidified biowastes were oven-dried at 65°C for 48 h and stored in sealed containers at room temperature.

In this study, we chose a nutrient-poor soil (a sandy loam, Luvisol, FAO), sampled from the negative control plot of the long-term CRUCIAL trial from the university of Copenhagen (for more details, see López-Rayo et al. 2016 and Lemming et al. 2019). This plot has not been fertilised since 2003 and was primarily used for cultivating spring cereals.

After sampling, the soil was air-dried and sieved through a 4-mm mesh. Prior to each incubation, the soil was brought to a moisture level of 45% of its water holding capacity (30 g 100 g^{-1}) and pre-incubated at 15°C for 2 weeks to reactivate the microbial community (Oehl et al. 2004). The pre-incubated soil is hereafter called 'T0', representing the soil just before the beginning of each incubation. The soil composition at time zero (T0) is presented in Table 1.

2.2 | Experimental Setup

In the experimental setup, incubations were performed in a system similar to the methodology described by Sica, Kopp, Müller-Stöver, et al. (2023). This setup consists of a 2-mm fertiliser layer that is incubated between two soil columns. The 2-mm fertiliser layer was chosen on the basis of preliminary studies carried out by Sica, Kopp, Müller-Stöver, et al. (2023), with the aim of allowing an appropriate amount of biowaste to be used in this study and ensuring full contact between the fertiliser layer and the soil interface on both sides. This system is designed to evaluate soil

13652389, 2025, 2, Downloaded from https://bsssjournals.onlinelibrary.wiley.com/doi/10.1111/ejss.70076 by Capes, Wiley Online Library on [17/03/2025]. See the Terms and Conditions (https://onlinelibrary.wiley.com/terms-and-conditions) on Wiley Online Library for rules of use; OA articles are governed by the applicable Creative Commons License

TABLE 1 | Soil, biogas digestate solid fraction (DSF) and meat and bone meal (MBM) untreated and acidified, respectively, and triple superphosphate (TSP) sulphur (S), carbon (C), nitrogen (N), and phosphorus (P) contents, the amount applied in each incubation, and the variation in the soil after 12 days of incubation. This table also provides the biowastes resin P (in % of total P), δ^{18}O-P, and pH before and after acidification.

		S	C	N	P	δ^{18}O	Resin-P	Organic-P	
		mg g^{-1}				‰	% of the total P		pH
Soil and fertilisers' composition									
	Soil T0	0.21	13	16	0.51	14.6	0.8	25	6.6
	TSP	—	—	—	208	21.7	73	0	—
DSF	Untreated	9.1	340	26.5	34.0	15.7	14	13.6	9.1
	Acidified	112	271	20.6	28.7	15.7	59	9.7	1.6
MBM	Untreated	4.9	428	98.4	34.2	12.1	2.3	12.6	5.8
	Acidified	41.7	401	90.3	28.6	12.1	82	9.3	3.9
Total amount applied (mg)									
	TSP	—	—	—	100	—	73	0	—
DSF	Untreated	4.3	1000	78	100	—	14	13.6	—
	Acidified	329	944	72	100	—	59	9.7	—
MBM	Untreated	17.1	1251	288	100	—	2.3	12.6	—
	Acidified	122	1402	316	100	—	82	9.3	—

Note: Total S and P determined by ICP-OES (Agilent 5100) and C and N by an elemental analyser (Vario macro cube, Elementar Analysensysteme GmbH, Germany).

P movement perpendicular to the fertiliser layer (in one dimension), which allows the sampling and analysis of soil layers at different distances from the fertiliser layer. Each experimental unit (soil column) consisted of two PVC discs: the first PVC disc (60 mm diameter × 18 mm height, total volume: 50.9 cm^3) filled with soil at 60% of its water-holding capacity (WHC), packed to a bulk density of 1.3 g cm^{-3} (66 g of dried soil). The second disc was also filled with soil up to 16 mm (45.2 cm^3, 58.8 g of dried soil). The 2-mm fertiliser layer was placed on top of the second disc and a 45 µm nylon mesh was used to prevent direct contact between the fertiliser placement layer and the soil (Figure 1a).

The total amount of fertiliser applied was calculated based on the total P content with the goal of achieving 100 mg of total P per experimental unit. The amount of C, N, and S applied is represented in Table 1. The soil discs were kept together with tape (Figure 1a,c). The columns were incubated in the vertical position inside sealed jars and glasses together with a 20 mL container filled with water (Figure 1b) in an incubator at 15°C. This temperature represents the average temperature during the Danish summer and is commonly used in studies to mimic these environmental conditions. For the negative control, the same procedure was followed, but no fertiliser was applied between the soil discs. For the analyses of the negative control, the soil was homogenised after incubation, and a subsample was collected from each experimental unit.

After 12 days of incubation, the soil discs were separated and inserted into a specially designed slicing piston that moves the soil column 1 mm upward with each 360° rotation (Figure 1c). For this study, the soil was sliced into 2 mm layers. For each experimental unit, at each distance from the fertiliser, two layers were obtained from the discs. These layers were thoroughly mixed with their corresponding layers from the other disc before conducting the analyses. The same experimental procedure was repeated four times, aiming to provide enough material for all analyses.

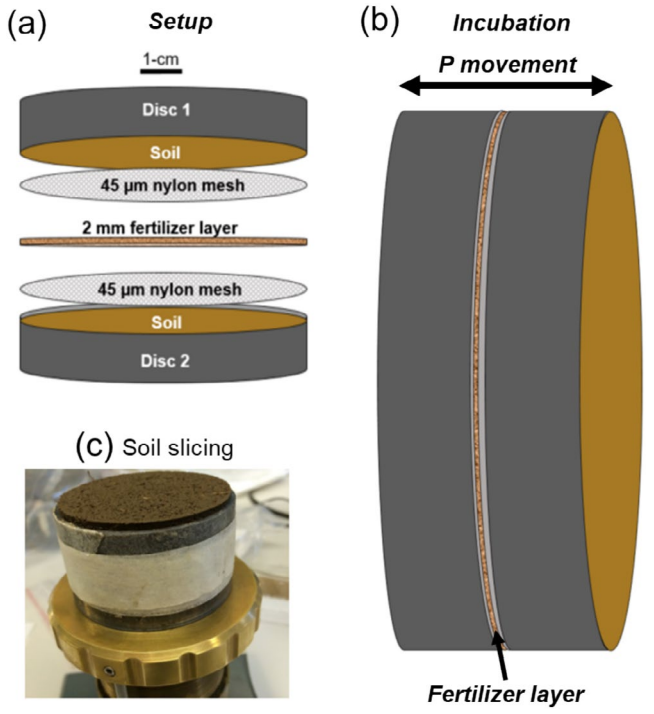

FIGURE 1 | Overview of the experimental setup (a), demonstrating the fertiliser layer incubated between two soil discs, with the P moving from the fertiliser layer through the soil discs (b), and the soil slicing of 2 mm soil layers to assess P movement through the soil (adapted from Sica et al. 2023).

13652389, 2025, 2, Downloaded from https://bsssjournals.onlinelibrary.wiley.com/doi/10.1111/ejss.70076 by Capes, Wiley Online Library on [17/03/2025]. See the Terms and Conditions (https://onlinelibrary.wiley.com/terms-and-conditions) on Wiley Online Library for rules of use; OA articles are governed by the applicable Creative Commons License

All incubation experiments were conducted under the same controlled conditions and treatments. An overview of the experimental setup can be seen in Figure 1 and Table 2.

2.3 | $\delta^{18}O$ In Phosphates of Soils and Fertilisers (Incubation 1)

After the pre-incubation, ^{18}O enriched water [$\delta^{18}O = +70‰$] (Sercon Limited, Crewe, UK) was applied to increase the soil moisture from 45% to 60% of its WHC. The soil at time zero (T0) had a water $\delta^{18}O$ value of −10‰, while for the incubated soils, the water $\delta^{18}O$ value was increased to +10.3‰. The expected isotopic equilibrium of oxygen in phosphate with soil water at T0 was +13.6‰, and + 30.9‰ for the soils with labelled water. The expected isotopic equilibrium values were calculated according to the following equation (Chang and Blake 2015):

$$P_{ws} = e^{\left[\left(\frac{14.43}{T}\right)-\left(\frac{26.54}{1000}\right)\right]} \times \left(\delta^{18}O_{soilwater} + 1000\right) - 1000 \quad (1)$$

where P_{ws} is the expected $\delta^{18}O$ value at equilibrium with soil water (in ‰), T is the incubation temperature (in Kelvin), and $\delta^{18}O_{soilwater}$ is the soil water $\delta^{18}O$ value (in ‰). More information about Equation (1) can be found in Chang and Blake (2015).

Extraction for resin-P followed a 1:10 ratio (wv^{-1}) and for resin+hexanol-P, the 1:10 ratio consisted of 9 mL of water and 1 mL of hexanol for each gram of dried soil. The samples were shaken in a horizontal shaker for 16 h in a cold room at 4°C. The amounts of fertiliser and soil extracted were adjusted based on preliminary tests to ensure a minimum of 930 μg of P per replicate. After extraction, anion exchange resins were eluted for 2 h in a 0.1 M NaCl + 0.1 M HCl using an end-over-end shaker. The orthophosphate in solution was determined by a flow injection analyser (FIAstar 5000, Foss Analytical, Denmark), using the ammonium molybdate blue method, measured at 720 nm.

The $\delta^{18}O$-P was determined for: (i) resin-P of the five fertilisers; (ii) resin-P and resin–hexanol P of the soil at T0, negative control, and fertilised soils at 0–2 and 4–6 mm from the fertiliser layer (Table 2).

The extracts were filtered sequentially through a glass fibre membrane and a 0.45 μm cellulose membrane, using a vacuum pump. The filtered samples were mixed with DAX resin, shaken for 2 h and filtered again with a glass fibre membrane to remove organic matter. For the meat and bone meal extracts, the DAX resin steps were repeated twice. The DAX resin was conditioned by shaking with methanol for 16 h and rinsed at least three times with milli-Q water before use. Based on the P contents (Table S2), an aliquot of each experimental unit was taken, the volume was determined aiming to an amount of 620 μg of P. If needed, the samples were concentrated to a volume < 10 mL in a water bath at 65°C. The protocol used to purify to obtain Ag_3PO_4 from the extracted phosphates from soils and the fertilisers for isotope analysis is described by Rieckmann et al. (2024). The Ag_3PO_4 samples were vacuum-roasted before analysis to remove intracrystalline water and co-precipitated O-bearing contaminants (Rieckmann et al. 2024).

TABLE 2 | Overview of the analyses performed in each incubation conducted in this study. All incubations were performed under the same conditions with the same treatments.

Incubation 1	
Soil slices	0–2 and 4–6 mm from the fertiliser layer
Analyses	Resin-P, Microbial-P and $\delta^{18}O$
Extraction ratio	1:10
Incubation 2	
Figures/Tables	Figure 2 and Table S2
Soil slices	0–2 and 4–6 mm from the fertiliser layer
Analyses	Hedley (1:60) and Inorganic N (1:5)
Table	Table S3
Incubation 3	
Soil slices	0–2, 2–4, 4–6, 6–8, 8–10, 10–12 mm from the fertiliser layer
Analyses	Resin-P, Microbial-P (1:10) and pH
Figures	Figures 5, 6, and 7
Incubation 4	
Soil	Bulk soil: both discs homogenised
Analyses	Respiration, ICP-OES and elemental analyser: P, S, C, and N; P release and mass balance
Tables	Table 3 and Figure 4

Stable oxygen isotopes of Ag_3PO_4 were measured on TC/EA PYRO Cube (Elementar, Hanau, Germany) coupled in continuous flow to an Isoprime100 isotope ratio mass spectrometer (IRMS)—(Isoprime100, Elementar, Manchester, UK). Samples of 0.3–0.32 mg Ag_3PO_4 were packed into high-purity silver capsules and introduced into a 60°C heated autosampler (Elementar, Hanau, Germany) and the pyrolysis tube was set at 1450°C. Samples of in-house Ag_3PO_4 were used to correct for linearity and drift. Measured $\delta^{18}O$ values were checked against certified reference material IAEA-601 (Benzoic acid, IAEA-International Atomic Energy Agency, Vienna, Austria), a reference Ag_3PO_4 purchased from Elemental Analytics (B2207, UK), and the in-house Ag_3PO_4 standard. Delta values are reported with respect to VSMOW and presented in ‰ notation. The analytical error of replicate analyses of standards was better than ±0.3‰.

The $\delta^{18}O$ composition of the phosphate in the microbial-P was calculated with a mass balance, according to Tamburini et al. (2012), in Equation (2) below:

$$\delta^{18}OP_{mic} = \frac{\left(\delta^{18}O - P_{hex} \times P_{hex}\right) - \left(\delta^{18}O - P_{resin} \times P_{resin}\right)}{\left(P_{hex} - P_{resin}\right)} \quad (2)$$

where $\delta^{18}OP_{mic}$ is the microbial P $\delta^{18}O$ (‰), $\delta^{18}O$-P_{hex} and $\delta^{18}O$-P_{resin} are the isotopic values of resin-P + hexanol and resin-P $\delta^{18}O$ (‰), respectively, and P_{hex} and P_{resin} are the resin-P plus

13652389, 2025, 2, Downloaded from https://bsssjournals.onlinelibrary.wiley.com/doi/10.1111/ejss.70076 by Capes, Wiley Online Library on [17/03/2025]. See the Terms and Conditions (https://onlinelibrary.wiley.com/terms-and-conditions) on Wiley Online Library for rules of use; OA articles are governed by the applicable Creative Commons License

hexanol and the resin-P concentrations in the extracts, respectively. More information about Equation (2) can be found in Tamburini et al. (2012).

The incorporation of ^{18}O into the phosphate from resin-P and microbial-P pools was calculated according to Liang and Blake (2006), using the following equation:

$$\text{Incorporation of}^{18}\text{O}\,(\%) = \frac{100 \times \left(\delta^{18}\text{O} - \text{Pt1} - \delta^{18}\text{O} - \text{Pt0}\right)}{\left(\delta^{18}\text{Osoilwatert1} - \delta^{18}\text{Osoilwatert0}\right)} \quad (3)$$

This calculation was made based on the differences in the soil resin-P and microbial-P $\delta^{18}O$ at the end and start of the experiment ($\delta^{18}O\text{-}P_{t1}$—$\delta^{18}O\text{-}P_{t0}$), divided by the difference between soil water $\delta^{18}O$ at the end and start of the experiment ($\delta^{18}O_{soilwatert1}$—$\delta^{18}O_{soilwatert0}$), where the $\delta^{18}O_{soilwatert1}$ and $\delta^{18}O_{soilwatert0}$ were +10.3‰ and −10‰, respectively. More information about Equation (3) can be found in Liang and Blake (2006).

2.3.1 | Isotopic Source Proportional Contributions

The source proportional contribution for resin-P and microbial-P at T1 was calculated using stable isotope mixing models. For microbial-P, two isotopic sources were assumed: soil microbial-P at T0 and intracellular phosphate at isotopic equilibrium with water, as driven by pyrophosphatase ($\delta^{18}OEq_{watersoil}$). Their proportional contribution was calculated using the following equation:

$$100 \times \delta^{18}\text{O} - \text{P}_{mic} = \left(x \times \delta^{18}\text{O}_{soilmicPt0}\right) + \left(y \times \delta^{18}\text{OEq}_{watersoil}\right) \quad (4)$$

where $\delta^{18}O\text{-}P_{mic}$ is the $\delta^{18}O$ of the soil microbial-P for a certain treatment (in ‰ notation), $\delta^{18}O_{soilmicPT0}$ is the soil microbial-P $\delta^{18}O$ at the beginning of the experiment (+8.6‰), and the $\delta^{18}O\text{-}Eq_{watersoil}$ is the expected isotopic equilibrium of oxygen in phosphate with soil water (+30.9‰; Equation 1). The proportional contribution of soil microbial-P and $\delta^{18}OEq_{watersoil}$ are represented by x and y, respectively ($x + y = 100$).

For soil resin-P, three isotopic sources were assumed: fertiliser, $\delta^{18}O$-Eq, and soil resin-P at T0. The software IsoSource 1.3 was used to perform the isotope mixing model and determine the range of proportional contributions for each of the three sources, according to the model represented in the following equation:

$$\begin{aligned} &100 \times \delta^{18}\text{O} - \text{P}_{resin} \\ &= \left(x \times \delta^{18}\text{O} - \text{P}_{soilresinPt0}\right) + \left(y \times \delta^{18}\text{O}_{fertiliser}\right) \\ &+ \left(z \times \delta^{18}\text{O} - \text{Eq}_{watersoil}\right) \end{aligned} \quad (5)$$

where $\delta^{18}O\text{-}P_{resin}$ is the $\delta^{18}O$ of the soil resin-P for a certain treatment (in ‰ notation), $\delta^{18}O_{soilresinPT0}$ is the soil resin-P $\delta^{18}O$ at T0 (+14.6‰), the $\delta^{18}O_{fertiliser}$ is the $\delta^{18}O$ of the fertiliser applied to the specific treatment, and the $\delta^{18}OEq_{watersoil}$ is the expected isotopic equilibrium of oxygen in phosphate with soil water, $\delta^{18}O\text{-}Eq_{watersoil}$ (+30.9‰, Equation 1). The proportional contributions of soil resin-P, the fertiliser, and $\delta^{18}OEq_{watersoil}$ are represented by x, y, and z, respectively ($x + y + z = 100$).

For the acidified DSF, the soil resin-P $\delta^{18}O$ was lower than the $\delta^{18}O$ of the three sources assumed, and the soil pH dropped to ~4; therefore, we assumed that it may have dissolved or exchanged P with the HCl-P pool. Thus, we assumed the HCl-P pool as a fourth source, with the $\delta^{18}O$ for the soil used in this study being previously determined as +10.8‰.

2.4 | Sequential Extractions (Incubation 2)

The sequential extractions, adapted from Hedley et al. (1982) were performed in triplicates on soil slices of 0–2 and 4–6 mm from the fertiliser layer (Table 2). This methodology helps assess the potential impact of treatments on soil P availability and responses at different distances from the fertiliser layer. Shortly, an equivalent of 0.5 g of dried soil was added to a 50 mL centrifuge tube and was sequentially extracted with: (1) anion exchange resin; (2) 0.5 M $NaHCO_3$; (3) 0.1 M NaOH; and (4) HCl. For each step, the extraction was performed in a 1:60 ratio by shaking for 16 h in an end-over-end shaker. For the first step, the anion exchange resins were carefully removed from the tubes, rinsed with Milli-Q water, and eluted in 0.1 M HCl by shaking in an end-over-end shaker for 2 h. After that, the falcon tubes were centrifuged at 7000 rpm for 10 min, and the supernatant was discarded. For steps 2, 3, and 4, samples were centrifuged at 7000 rpm for 10 min and filtered through Whatman filter papers (number 5). The ortho-phosphate in solution was determined by a flow injection analyser (FIAstar 5000, Foss Analytical, Denmark), using the ammonium molybdate blue method, measured at 720 nm.

The total P of the resin-P, $NaHCO_3$-P, and NaOH-P pools was determined by digesting the extracts with 2.5 M H_2SO_4 and potassium persulphate in Pyrex tubes at 110°C for 60 min. After that, the tubes were removed, cooled down, and 10% NaOH solution was added to each tube, and total P, as orthophosphate, was measured as described above. Organic P was determined as the difference between total P and inorganic P. This method was adapted from Ebina et al. (1983).

2.5 | P Movement in the Soil—pH, Resin, and Microbial P (Incubation 3)

Soils were sliced at 0–2, 2–4, 4–6, 6–8, 8–10, and 10–12 mm from the fertiliser layer. For each distance, resin-P, microbial-P, and pH were determined (Table 2). Resin-P is considered a proxy for abiotic P movement in the soil, while microbial-P is a proxy for P movement via microbial pathways. The pH is relevant to demonstrate the effects of the placement of untreated and acidified biowaste on chemical processes in the soil, and it will also affect P solubility. For the pH, the soil was shaken with Milli-Q water at a 1:5 ratio in falcon tubes for 1 h. For resin-P and microbial-P, each sample was split into two subsamples equivalent to 3 g of dried soil. The subsamples were extracted as follows: (1) resin-P: 1:10 ratio, with one anion exchange membrane added for each gram of dried soil; (2) resin + hexanol: 1:10 ratio, with one anion exchange membrane added for each gram of soil, and 27 mL of Milli-Q water plus 3 mL of hexanol. Microbial-P was determined as the difference between the P_{hex} and P_{resin} subsamples and by

13652389, 2025, 2, Downloaded from https://bsssjournals.onlinelibrary.wiley.com/doi/10.1111/ejss.70076 by Capes, Wiley Online Library on [17/03/2025]. See the Terms and Conditions (https://onlinelibrary.wiley.com/terms-and-conditions) on Wiley Online Library for rules of use; OA articles are governed by the applicable Creative Commons License

the soil P sorption correction factor (Bünemann et al. 2016), according to the following equation:

$$P_{mic} = \frac{(P_{hex} - P_{resin})}{\text{P sorption correction factor}} \quad (6)$$

where P_{mic} is in mg kg soil^{-1}, the P_{hex} and P_{resin} were determined in mg kg soil^{-1}, as previously described, and the P sorption capacity of the soil was used as a correction factor (in %) and was determined by applying P spiking solutions in a third independent resin extraction and calculated as the difference between the measured value and the spike (NSW 1995; Sica, Kopp, Müller-Stöver, et al. 2023).

The 3-parameter exponential decay equation (Equation 7) is used to model water-extractable P diffusion in the soil (Hao et al. 2002). In this study, it was adapted, and this equation was used to fit the curves for the resin-P and microbial-P movement in the soil, as represented in Equation (7):

$$y = a \times e^{-bx} + y0 \quad (7)$$

where y is the resin-P or microbial-P concentration at a certain distance from the biowaste layer (mg kg soil^{-1}); x is the distance from the biomaterial layer (mm); $y0$ is the soil background (mg kg soil^{-1}); a and b are obtained by fitting the data in Equation (7), with b representing the slope of the curve.

2.6 | Total P, S, C, and N in the Soil (Incubation 4)

The C and N contents were determined by an elemental analyser (Vario macro cube, Elementar Analysensysteme GmbH, Germany). The P and S contents were determined by ICP-OES (Agilent 5100) after microwave digestion with HNO_3, H_2O_2, and HF.

The total P released from the fertiliser to the soil was calculated according to Equation (8):

$$P \text{ released } (\%) = 100 \times \frac{(\text{Total amount of P after incubation} - \text{Total amount of P } t0)}{\text{Total amount of P applied}} \quad (8)$$

which represents the difference in the total P in the soil before and after incubation in mg, divided by the total P applied (100 mg).

The apparent recovery determined the percentage of the total P applied that was recovered in the different P pools from the Hedley sequential extraction in the bulk soil and the microbial-P in the first 12 mm of soil from the placement zone and was calculated as in the following equation:

$$\text{Apparent recovery } (\%) = 100 \times \frac{(\text{Total amount of microbial or resin} - \text{P at } 0-12 \text{ mm} - \text{total amount P neg.})}{\text{total amount of P applied}}. \quad (9)$$

where the total amount of P in the P pools of the bulk soil and microbial-P at the 0–12 mm from the fertiliser layer (in mg) and the negative control (Neg.) respective values are divided by the total amount of P applied (100 mg).

2.7 | Soil Respiration

The soil respiration was measured by adding 10 mL of 1 M NaOH to a plastic container placed inside a sealed jars containing its respective experimental unit. The NaOH samples were collected at 6 and 12 days of incubation. Barium chloride and phenolphthalein were added to the NaOH solution. After that, the NaOH solution was titrated with 1 M HCl, and respired CO_2 (mg per kg of soil) was calculated following Alef (1995). Linear regressions and Pearson correlations were performed to assess the correlation between the microbial respiration and the ^{18}O incorporation from water into the resin-P and microbial-P. Since the soil was sieved and there was no presence of mesofauna or plant roots, the CO_2 released during the incubations can be considered as coming mainly or exclusively from soil respiration and, therefore, derived from microbial activity.

2.8 | Statistics

The statistical analyses were performed on IBM SPSS Statistics 27.0, conducting one-way ANOVA. Data homogeneity of

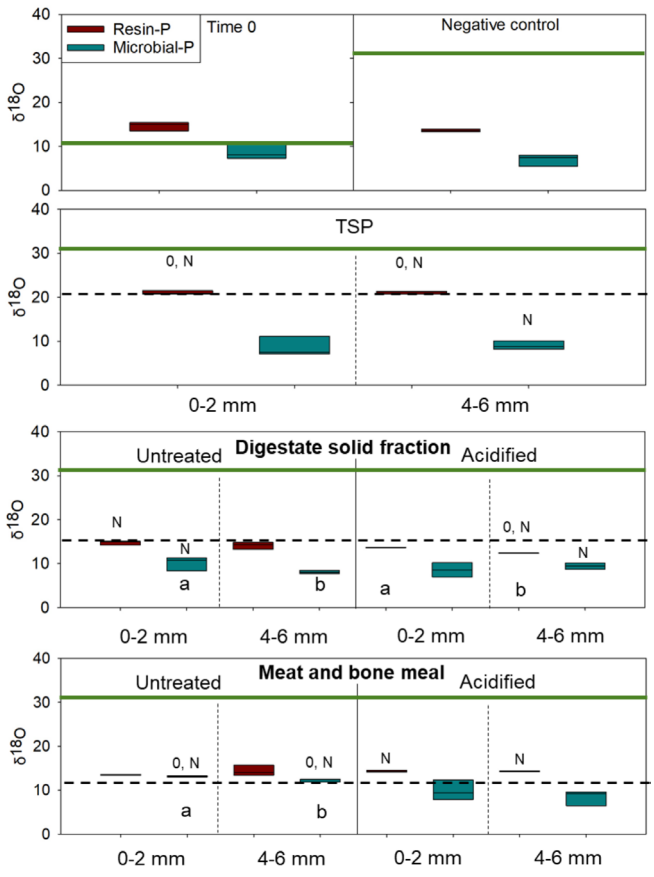

FIGURE 2 | $\delta^{18}O_{Resin\text{-}P}$ and $\delta^{18}O_{Microbial\text{-}P}$ values of the soil at different distances (0–2 and 4–6 mm) from the fertiliser layer after 12 days of incubation. Dashed lines represent the fertiliser $\delta^{18}O_{Resin\text{-}P}$ s before being applied to the soil and solid (dark green) lines represent the expected $\delta^{18}O$ value of phosphate in equilibrium with soil water ($n = 3$). TSP: Triple super phosphate; Time 0: Soil before incubation; Negative control: Soil incubated for 12 days with no fertiliser applied. 0 indicate a significant different to Time zero, N to the negative control (Dunnet's test, <0.05). Different letters indicate a significant different between distances (T test, <0.05).

13652389, 2025, 2, Downloaded from https://bsssjournals.onlinelibrary.wiley.com/doi/10.1111/ejss.70076 by Capes, Wiley Online Library on [17/03/2025]. See the Terms and Conditions (https://onlinelibrary.wiley.com/terms-and-conditions) on Wiley Online Library for rules of use; OA articles are governed by the applicable Creative Commons License

TABLE 3 | Microbial respiration at 0–6, 6–12 days of incubation (also total), total C, N, P, and S contents released from the fertiliser to the soil, soil and fertiliser layer pH, and soil resin-P after 12 days of incubation.

		Respiration (mg CO_2 kg soil $^{-1}$)	Content (mg kg soil^{-1})			Inorganic N (mg kg soil $^{-1}$)			
			Total N	Total C	Total S	$N–NO_3^-$		$N–NO_4^+$	
	Neg.	4.73 ± 0.5	1600 ± 10	13,466 ± 144	210 ± 26	—	—	—	—
	TSP	20 ± 2.5^{N}	1689 ± 95	13,500 ± 45	243 ± 10	11.1 ± 0.2		17.7 ± 0.5	
DSF	Untreated	34.3^{a} ± 0.5^{N}	1700 ± 47	13,833 ± 593	275^{b} ± 9	11.2 ± 1.4	5.3 ± 0.4	3.4 ± 0.1	3.1 ± 0.1
	Acidified	5.91^{b} ± 1.0	1766 ± 55	12,700 ± 492	1071^{a} ± 23^{N}	39 ± 3.2	18 ± 1.9	3.4 ± 0.1	2.7 ± 0.1
MBM	Untreated	500^{a} ± 14^{N}	2299 ± 38^{N}	15,233 ± 144^{N}	289^{b} ± 23	436 ± 8	454 ± 9.9	21.6 ± 2	15.9 ± 2
	Acidified	357^{b} ± 5^{N}	2467 ± 98^{N}	15,566 ± 733^{N}	585^{a} ± 39^{N}	469 ± 9	498 ± 3	15.3 ± 0.2	17.2 ± 2.1

Note: Different letters indicate a significant difference between untreated and acidified biowastes (T test < 0.05); ^{N}A significant difference to the negative control; ^{0}A significant difference to T0. ± after the averages indicate the standard errors ($n = 3$).
Abbreviations: DSF: digestate solid fraction; MBM: meat and bone meal; Neg.: negative control with soil incubated for 12 days with no fertiliser applied; TSP: triple superphosphate.

variance was validated through Levene's test, and normal distribution was verified via the Kolmogorov–Smirnov test. Differences in P movement and soil pH (Figures 3 and 4) were evaluated using Tukey's HSD test ($p < 0.05$). For parameters involving two distances (0–2 vs. 4–6 mm) or acidification effects (untreated vs. acidified), a t test was applied (< 0.05). The TSP treatment was used as a reference, and the biowastes were not statistically compared to it. Specific parameter-related statistical descriptions were included in the captions of respective graphs and figures. Graphs were generated using SigmaPlot version 14.0.

3 | Results

3.1 | $\delta^{18}O$ In Phosphate

After the pre-incubation period, at T0, the soil resin $\delta^{18}O$-P value closely matched the calculated equilibrium value of +13.6‰. However, following a 12-day incubation with ^{18}O enriched water, none of the treatments showed a $\delta^{18}O$-P values approaching the equilibrium value of +33.6‰. Notably, in the negative control, both the resin-P and microbial-P $\delta^{18}O$ decreased during incubation (from +14.6 at T0 to +13.6‰ and from +8.6 to +7.0‰, respectively); however, no significant difference was observed in comparison to their respective $\delta^{18}O$-P values at T0. For the TSP, the soil resin $\delta^{18}O$-P values at 0–2 and 4–6 mm from the fertiliser layer significantly increased compared to the resin-P at T0 and the negative control, reaching a similar value to the TSP resin-P $\delta^{18}O$ value of +21.7‰. The microbial $\delta^{18}O$-P value at 4–6 mm was +9.0‰, significantly greater than the negative control (Figure 2).

For the DSF-untreated, the resin-P (+14.7‰) and microbial-P (+10.1‰) $\delta^{18}O$-P values were significantly greater than the negative control at 0–2 mm from the fertiliser layer. The microbial $\delta^{18}O$-P value was significantly less at 4–6 mm (+8.0‰) from the fertiliser layer compared to the 0–2 mm soil. For DSF-acidified, the resin $\delta^{18}O$-P value at 0–2 mm (+13.6‰) was significantly greater than at 4–6 mm. At both distances, the resin $\delta^{18}O$-P value was less than the fertiliser resin $\delta^{18}O$-P value (+16‰). The resin $\delta^{18}O$-P value at 4–6 mm (+12.3‰) was significantly less than the T0 and the negative control, whereas the microbial-P at 4–6 mm (+9.4‰) was significantly greater than the negative control microbial $\delta^{18}O$-P value (Figure 2).

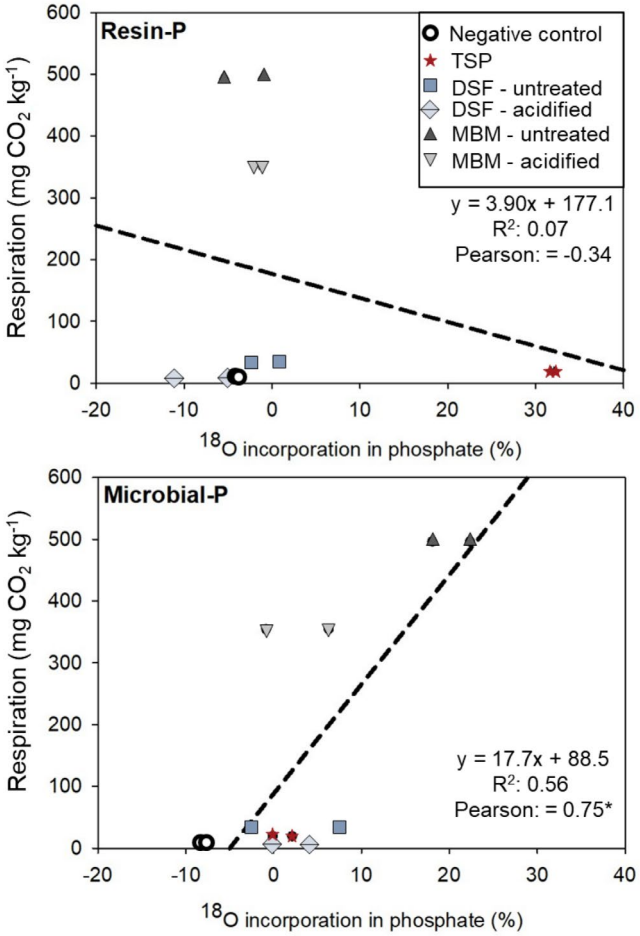

FIGURE 3 | Correlation between microbial respiration and ^{18}O incorporation in the resin-P (top) and microbial-P (bottom) pools after 12 days of incubation. DSF: digestate solid fraction; MBM: meat and bone meal; TSP: triple superphosphate. *Significant Pearson correlation for the microbial-P ($p = 0.004$).

13652389, 2025, 2, Downloaded from https://bsssjournals.onlinelibrary.wiley.com/doi/10.1111/ejss.70076 by Capes, Wiley Online Library on [17/03/2025]. See the Terms and Conditions (https://onlinelibrary.wiley.com/terms-and-conditions) on Wiley Online Library for rules of use; OA articles are governed by the applicable Creative Commons License

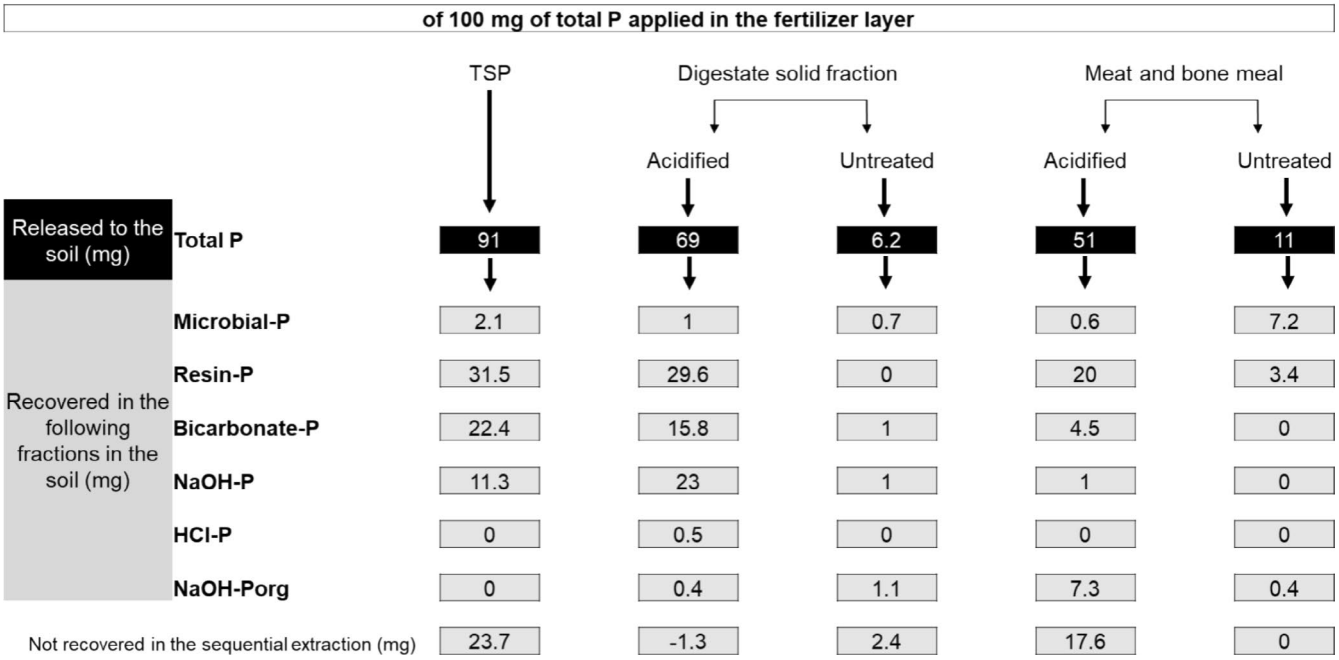

FIGURE 4 | Mass balance between P released from the fertiliser layer (total P applied 100 mg) and the soil pools (Hedley inorganic and organic, and microbial) where the released P was recovered. Only for TSP and acidified MBM was a considerable amount of P not recovered.

In the MBM-untreated treatment, the resin δ^{18}O-P values at both distances were greater than the fertiliser resin-P (+12.5‰). At both distances, microbial δ^{18}O-P values were close to the fertiliser's phosphate δ^{18}O and significantly greater than the T0 and negative control microbial-P. The microbial-P at 0–2 mm (+13.1‰) was significantly greater compared to the 4–6 mm microbial δ^{18}O-P (+12.3‰). For the MBM-acidified, the resin δ^{18}O-P values at both distances were 14.3‰ and significantly greater than the negative control (Figure 2).

Therefore, this study found that after 12 days of incubation with ^{18}O-enriched water, none of the treatments reached the expected isotopic equilibrium value of +33.6‰ for δ^{18}O-P. Despite this, treatments with TSP, DSF, and MBM showed significantly greater δ^{18}O-P values than the negative control, particularly near the fertiliser layer. Acidified treatments generally exhibited greater resin-P δ^{18}O values than untreated ones, though microbial δ^{18}O-P values varied across distances, with notable differences between treatments and the control. This suggests that both biotic and abiotic processes influenced P dynamics, with variations in P movement and microbial activity depending on fertiliser type and treatment.

3.2 | Soil Respiration and ^{18}O Incorporation

The DSF-acidified treatment was the only treatment that did not show a significant difference in cumulative microbial respiration after 12 days of incubation compared to the negative control and was significantly lower than DSF-untreated. The accumulated microbial respiration of MBM-untreated was the highest among treatments and significantly greater than MBM-acidified (Table 3). The microbial respiration showed a significant and positive correlation with the incorporation of soil water ^{18}O into microbial biomass P (Pearson = 0.751; $p < 0.04$). However, the correlation between ^{18}O incorporation into resin-P and respiration was not significant ($p = 0.874$) and tended to be negative (Pearson = −0.342) (Figure 3). In summary, the DSF-acidified treatment showed no significant difference in microbial respiration compared to the negative control, while MBM-untreated had the highest respiration, with a positive correlation between microbial respiration and ^{18}O incorporation into microbial biomass P, but not into resin-P.

3.3 | Isotope Source Proportional Contribution to Soil Phosphate δ^{18}O

After 12 days of incubation, for MBM-untreated, $\delta^{18}OEq_{watersoil}$ contributed to 19.9% and 15.9% of the microbial-P δ^{18}O value at 0–2 and 4–6 mm, respectively (Table S4). For soil resin-P, the fertiliser was the main source contributing to the TSP δ^{18}O-P value at both distances. For DSF-untreated at 0–2 mm and MBM-acidified and MBM-untreated at both distances, both the fertiliser and the initial soil resin-P were the main sources contributing to soil resin-P after incubation (T1). Whereas for DSF-untreated (4–6 mm) and DSF-acidified (both distances) the soil HCl-P pool at T0 was likely to be the main source contributing to the δ^{18}O-P value at the end of the incubation (Table S3). In summary, after 12 days of incubation, microbial δ^{18}O-P value in MBM-untreated was mainly influenced by $\delta^{18}OEq_{watersoil}$, while soil resin-P for TSP was mainly derived from fertiliser, and for DSF-untreated and MBM-acidified, both fertiliser and initial soil resin-P contributed significantly to resin-P levels.

3.4 | Phosphorus Distribution: Mass Balance and Pools

After 12 days of incubation, all treatments, including the negative control, exhibited a significant increase in the inorganic resin-P pool concentration compared to T0, notably TSP,

13652389, 2025, 2, Downloaded from https://bsssjournals.onlinelibrary.wiley.com/doi/10.1111/ejss.70076 by Capes, Wiley Online Library on [17/03/2025]. See the Terms and Conditions (https://onlinelibrary.wiley.com/terms-and-conditions) on Wiley Online Library for rules of use; OA articles are governed by the applicable Creative Commons License

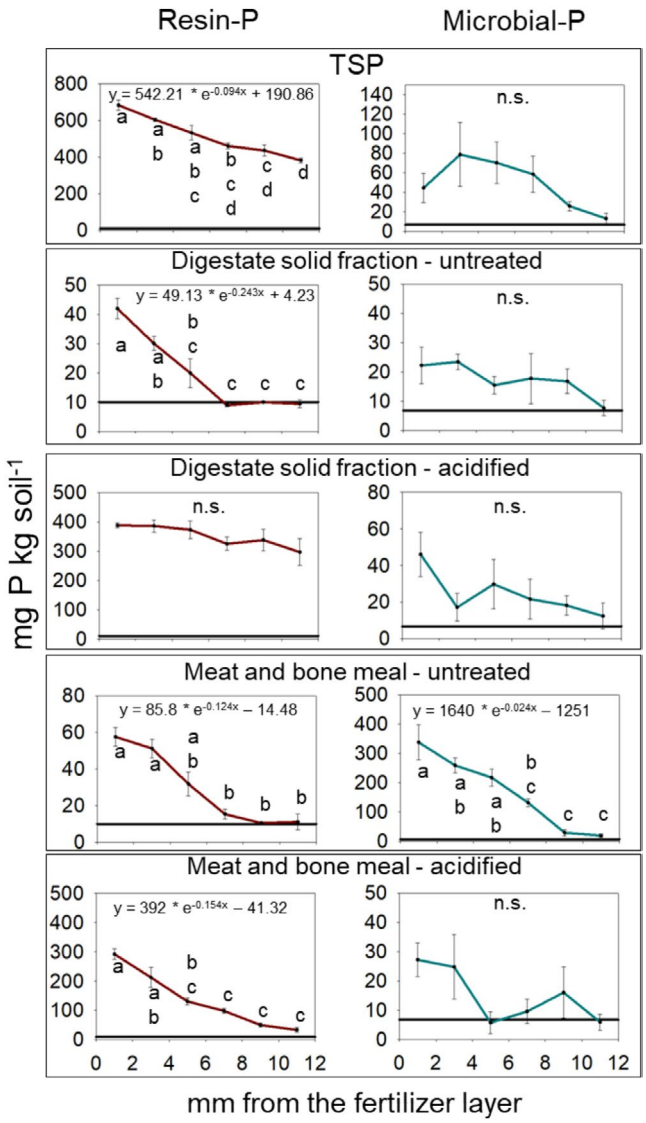

FIGURE 5 | Soil resin-P (left) and microbial-P (right) concentrations in mg P kg dry soil^{-1} (y axis) at different distances (0–2, 2–4, 4–6, 6–8, 8–10, and 10–12 mm) from the fertiliser layer (x axis) after 12 days of incubation. Solid lines represent the negative control resin-P and microbial-P. Error bars indicate the standard errors ($n = 3$). Different letters indicate a significant difference between distances (Tukey HSD < 0.05). n.s. indicate that there were no significant differences between distances. The three-parameter exponential decay equation is represented above the curves to which it was fitted. The equation is not represented in the cases where the curve did not fit. DSF: digestate solid fraction; MBM: meat and bone meal; TSP: triple super phosphate.

DSF-acidified, and MBM-acidified. These same treatments showed substantial increases in the inorganic $NaHCO_3$-P and NaOH-P pool concentrations at both distances, significantly higher than the negative control. For DSF-untreated and MBM-untreated treatments, both pools were significantly larger than T0 but had no difference to the negative control. NaOH organic P significantly increased compared to T0 and showed no difference from the negative control for all treatments, except for TSP at 0–2 mm, which was notably less than the negative control but not different from T0. However, none of the treatments led to a significant increase in the HCl-P pool compared to the negative control (Table S4).

After 12 days of incubation, 91% of the total P applied with TSP was released to the soil, with 31.5% being recovered in the resin-P and 33.7% recovered in the NaHCO3-P and NaOH-P pools. For both biowastes, acidification increased the total P released to the soil and the apparent recovery in the soil resin-P. However, for the MBM, acidification reduced the P recovered from the microbial biomass (Figure 4).

In summary, after 12 days of incubation, TSP, DSF-acidified, and MBM-acidified treatments significantly increased resin-P, $NaHCO_3$-P, and NaOH-P pools compared to T0 and the control, while acidification enhanced P release and recovery in the soil. However, MBM-acidified treatments reduced P recovery from microbial biomass, and no treatments increased the HCl-P pool.

3.5 | P Movement in the Soil

Figure 5 shows the resin-P and microbial-P at different distances from the fertiliser layer, indicating the abiotic and biotic P movement in the soil after 12 days of incubation. Except for DSF-acidified, significant differences between distances were observed across all fertilisers, indicating a characteristic diffusion pattern that fitted the three-parameter exponential decay curves. TSP, DSF-acidified, and MBM-acidified exhibited substantial resin-P concentrations at 0–2 mm (683, 387, and 292 mg P kg soil^{-1}, respectively), with resin-P levels persisting even at the farthest distance (9–11 mm) (391, 296, and 33,292 mg P kg soil^{-1}, respectively) (Figure 5).

In terms of microbial-P, high variability was evident among most fertilisers, with significant differences between distances only observed for MBM-untreated. The MBM-untreated treatment, the only one fitting the three-parameter exponential decay model, displayed the largest content ranging from 337 to 19 mg microbial-P kg soil^{-1} at 0–2 and 9–11 mm from the fertiliser layer, respectively (Figure 5).

MBM-acidified and MBM-untreated treatments displayed microbial growth within the fertiliser layer, as well as at the soil–fertiliser interface. Remarkably, for the MBM-untreated treatment, microbial growth was observed across the entire disc (Figure 6).

In summary, TSP, DSF-acidified, and MBM-acidified showed significant resin-P diffusion, with large concentrations near the fertiliser layer and persistence at farther distances. MBM-untreated had the greatest microbial-P content and exhibited microbial growth throughout the entire soil disc, unlike the other treatments.

3.6 | Soil pH

Figure 7 shows the pH of the 2-mm soil layers at different distances from the placement zone after 12 days of incubation. The DSF-acidified considerably decreased the soil pH from the

13652389, 2025, 2, Downloaded from https://bsssjournals.onlinelibrary.wiley.com/doi/10.1111/ejss.70076 by Capes, Wiley Online Library on [17/03/2025]. See the Terms and Conditions (https://onlinelibrary.wiley.com/terms-and-conditions) on Wiley Online Library for rules of use; OA articles are governed by the applicable Creative Commons License

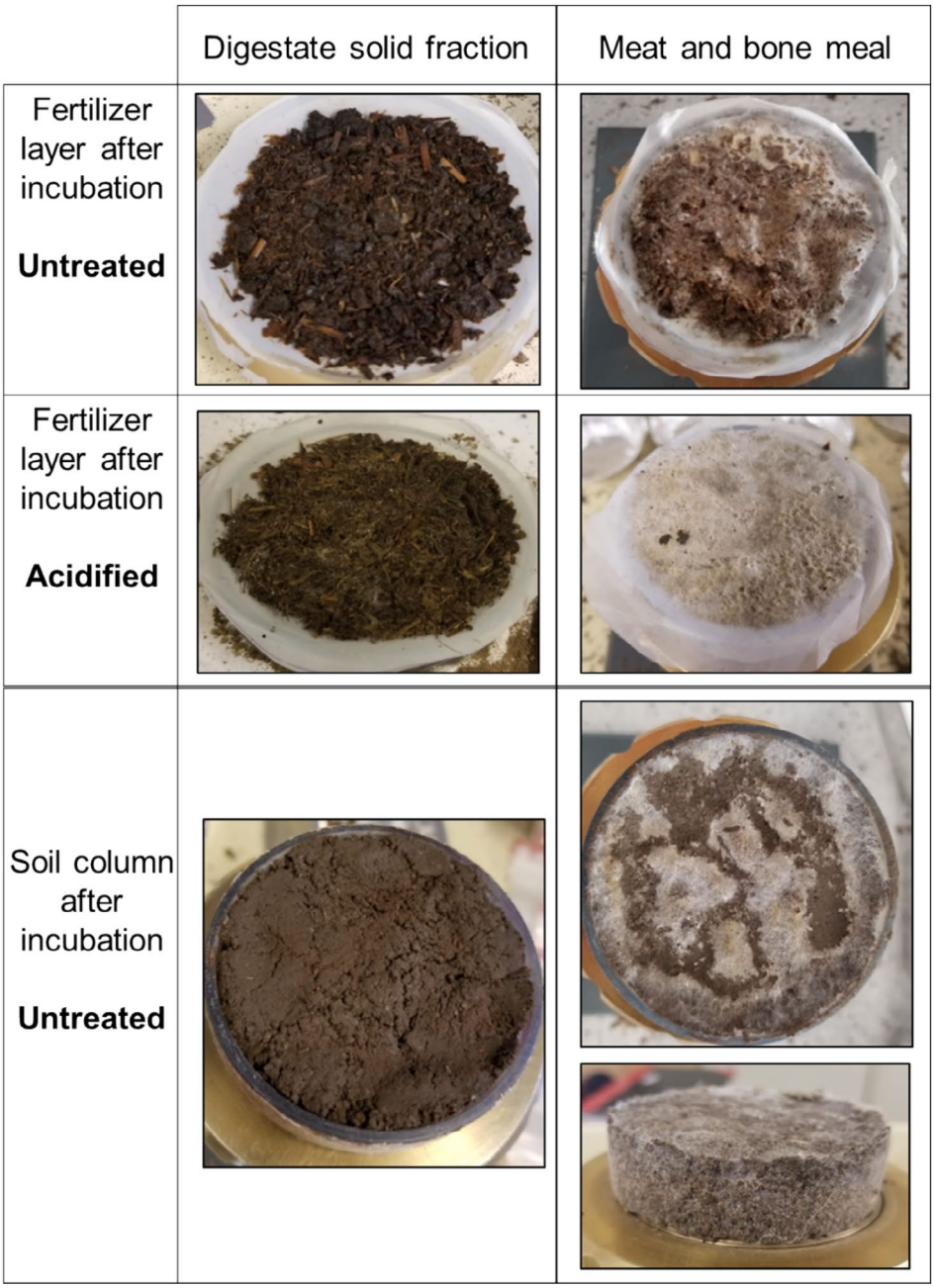

FIGURE 6 | Fertiliser layer with digestate solid fraction and meat and bone meal untreated and acidified, and soil columns of untreated biowaste after the incubation.

0–2 mm (3.45) to the 9–11 mm (4.54), compared to the initial soil pH (6.58), having a pH of 4.5 in the fertiliser layer after incubation. In contrast to it, the MBM-acidified and MBM-untreated showed an alkalinisation in the fertiliser layer (7.5 and 7.8, respectively), and in its surrounding soil (Figure 7).

3.7 | Nutrient Release to the Soil

The soil S content showed a significant increase only in the treatments with acidified biowastes, indicating the effect of acidification on S dynamics, as compared to the negative control, which showed no changes. In terms of total P content, the application of TSP and both acidified biowastes significantly increased soil P levels at all distances and the P release to the soil (Table 3). This increase highlights the potential of these treatments to improve P availability in the soil.

Both MBM treatments also caused a substantial rise in total C and N contents in the soil when compared to the negative control, further emphasising the nutrient enrichment and increase in microbial activity provided by MBM. Additionally, these treatments showed elevated ammonium concentrations at both 0–2 and 4–6 mm from the placement zone, indicating efficient N release from the biowaste. Despite this, the nitrate content remained consistently low for all treatments, with levels not exceeding 21.6 mg kg soil^{-1} (Table 3), suggesting limited nitrification or slow nitrogen conversion processes during the incubation period. This balance between ammonium and nitrate could have implications for plant nitrogen uptake and soil fertility management.

13652389, 2025, 2, Downloaded from https://bsssjournals.onlinelibrary.wiley.com/doi/10.1111/ejss.70076 by Capes, Wiley Online Library on [17/03/2025]. See the Terms and Conditions (https://onlinelibrary.wiley.com/terms-and-conditions) on Wiley Online Library for rules of use; OA articles are governed by the applicable Creative Commons License

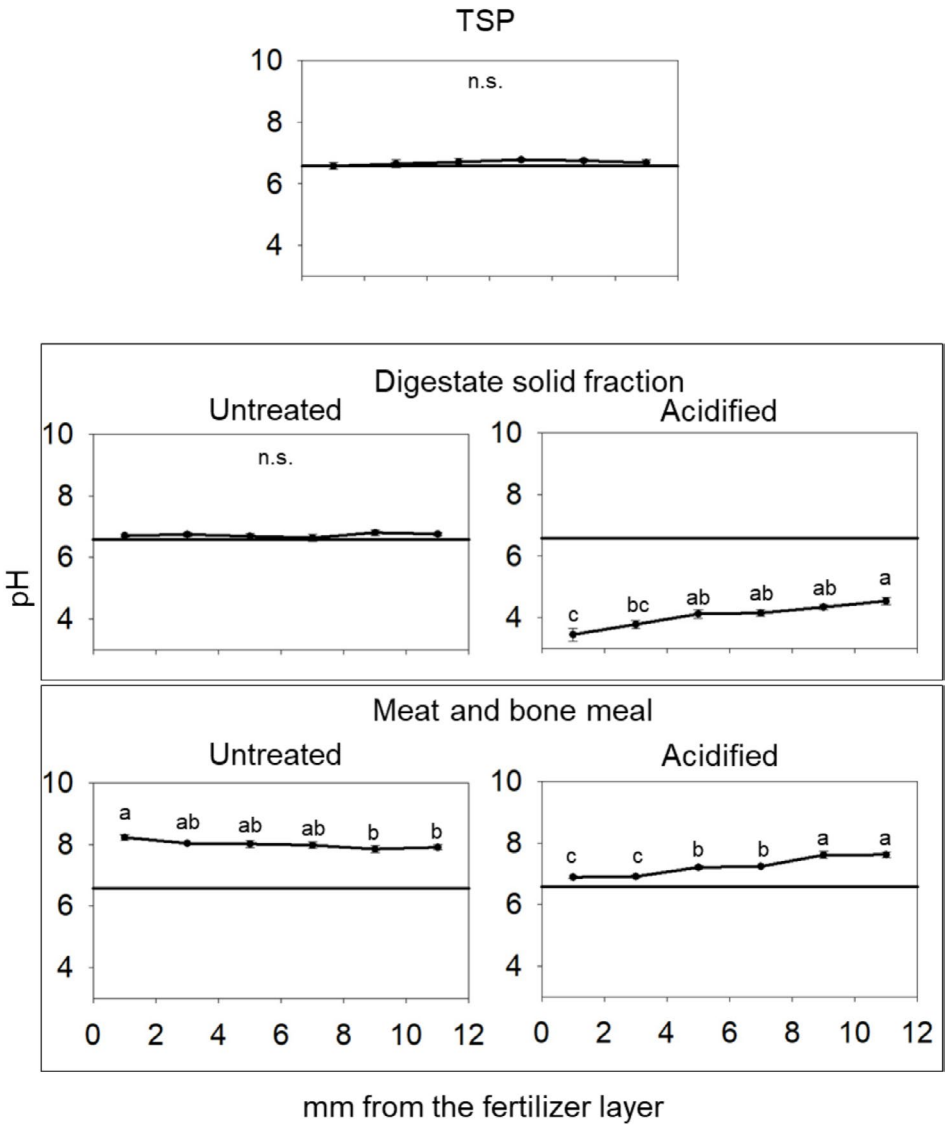

FIGURE 7 | Soil pH at different distances (0–2, 2–4, 4–6, 6–8, 8–10, and 10–12 mm) from the fertiliser layer after 12 days of incubation. Solid lines represent the negative control pH. Error bars indicate the standard errors ($n = 3$). Different letters indicate a significant difference between distances (Tukey HSD < 0.05). n.s. indicate that there were no significant differences between distances. DSF: digestate solid fraction; MBM: meat and bone meal; TSP: triple super phosphate.

4 | Discussion

4.1 | Chemical and Biological Changes in the Soil

4.1.1 | P Release to the Soil

In this study, acidification significantly increased the release of P from the biomaterial layer to the soil for both MBM and DSF. These results are consistent with those of Sica, Kopp, Müller-Stöver, et al. (2023), who reported that acidified MBM and digestate solid fraction released 36% and 77% of the total P to the soil, respectively, in only 12 days. However, these values were lower than those observed for TSP, which released 93% of the total P after 12 days. Sica, Kopp, Müller-Stöver, et al. (2023) also found a high correlation between the release of P from the fertiliser to the soil and the water-extractable P of the fertiliser. In this study, MBM-acidified was the fertiliser with the largest resin-P content before application to the soil (82% of total P), even exceeding that of TSP (73%). However, MBM-acidified released 51% of the total P applied to the soil, which was significantly less than DSF-acidified (69%) and TSP (93%).

Most of the P in MBM is derived from bones, primarily in the form of hydroxyapatite (Jeng et al. 2004, 2007), which can dissolve at a pH below 4.0 (Valsami-Jones et al. 1998; Sica, Kopp, Müller-Stöver, et al. 2023). The dissolution of hydroxyapatite, as observed with acidified MBM at pH 3.9, resulted in 82% of the total P being extracted by the resin. However, the pH of MBM acidified in the placement zone increased significantly during incubation, reaching 6.5 after 12 days. This pH increase may have favoured the precipitation of dissolved P with calcium, thereby reducing the amount of P released from the fertiliser layer into the soil. This was not the case for DA, which maintained a pH of 2.1 even after 12 days and released 69% of the total P applied.

13652389, 2025, 2, Downloaded from https://bsssjournals.onlinelibrary.wiley.com/doi/10.1111/ejss.70076 by Capes, Wiley Online Library on [17/03/2025]. See the Terms and Conditions (https://onlinelibrary.wiley.com/terms-and-conditions) on Wiley Online Library for rules of use; OA articles are governed by the applicable Creative Commons License

Therefore, as demonstrated by Sica and Magid (2024), acidification can increase the P release from biowastes in the early stages of plant growth, serving as an efficient starter fertiliser to boost plant and root growth. The remaining P in the placement zone may be able to sustain plant growth during the crop growing season.

4.1.2 | Soil Respiration and Soil C and N

Acidification did not affect total soil C and N for DSF, and no significant differences were observed compared to the negative control. During the solid–liquid separation process, most of the dissolved C and N remain in the liquid fraction (Chuda et al. 2021). As a result, the solid fraction contains more fibrous materials (Al Seadi et al. 2013), with more stable and recalcitrant forms of C, such as lignin and non-hydrolyzable lipids, resulting in a relatively higher C/N ratio of approximately 16 (Tambone et al. 2009; Al Seadi et al. 2013).

For these reasons, despite the application of relatively large amounts of C and N (~1000 and ~75 mg, respectively), the organic matter in DSF remains stable (Panuccio et al. 2021), likely resulting in less C and N release into the soil and relatively low microbial respiration during the incubation period. Acidification of DSF significantly reduced microbial respiration, with values as low as the negative control and significantly less than those for DSF untreated. This suggests that the low pH of the placement zone and soil, combined with the presence of more stable organic matter sources, created conditions that inhibited microbial growth during incubation.

Similar to DSF, the acidification of MBM did not affect the total C and N contents in the soil. However, MBM primarily consists of C and N derived from meat and blood, with high protein content and a low C/N ratio (Brod, Øgaard, Hansen, et al. 2015; Brod, Øgaard, Haraldsen, et al. 2015). This composition stimulates microbial activity and increases N mineralisation rates (Chaves et al. 2006). In this study, acidification reduced microbial respiration for both MBM and DSF; however, MBM-acidified microbial activity anyhow remained high compared to the negative control and TSP treatments. Additionally, for both MBM-acidified and MBM-untreated, the ammonium content in the soil at 0–2 and 4–6 mm was relatively high, above 430 mg kg^{-1}. Several studies have previously reported that a toxicity zone may develop in N-rich soil zones with ammonium contents exceeding 150–200 mg kg^{-1}. These high N contents can potentially damage seeds if applied too close, and the plant root tips, prevent root access to the fertiliser placement zone, and compromise crop growth in the early stages (Pan et al. 2016; Pedersen et al. 2020). However, it is expected that over time, ammonium will be converted into nitrate, reducing the toxic effect (Nkebiwe et al. 2017; Baral et al. 2021).

4.1.3 | pH

The placement of TSP and DSF-untreated did not have any effect on soil pH. However, significant differences were observed for DSF-acidified, MBM-acidified, and MBM-untreated. A similar increase in the soil pH for untreated and acidified meat and bone meal was also observed by Sica, Kopp, Müller-Stöver, et al. (2023). Our results indicate that for both MA and MU, there was a high rate of N mineralisation, accompanied by high ammonium contents; however, the nitrification rates appeared to be lower. In the soil, complex organic N undergoes a process of amminization, during which it is initially degraded into amines ($R–NH_2$). Subsequently, these amino acids undergo hydrolysis, resulting in the production of ammonium and hydroxide ions (Girkin and Cooper 2022). This contributes to the soil alkalization that we observed for both MBM-acidified and MBM-untreated, suggesting that biological processes were driving changes in soil pH.

In the case of DSF-acidified, the changes in soil pH were more likely due to chemical processes, as the soil pH was significantly reduced up to 10–12 mm from the placement zone, probably because of the release of protons from the acidified biomaterial layer into the soil, diffusing throughout the soil disc. The low pH in the acidified DSF placement zone (2.1) and surrounding soil (0–2 and 4–6 mm < 4) may create a barrier for root growth in the placement zone and its surrounding soil, as it can be negatively affected at a pH below 4.5 and completely inhibited when the soil pH is below 4 (Yan et al. 1992). As demonstrated by Sica and Magid (2024) compared to the untreated material, the placement of acidified digestate solid fraction significantly reduced root growth in the placement zone due to the low pH. However, it significantly increased the total root length in the soil surrounding the placement zone as well as the P and S uptake by broccoli, bean, pea, onion, and carrots at the early growth stages due to the increased P solubility and availability in the soil surrounding the placement zone.

4.2 | Soil P Fractionation

For TSP, DSF-acidified, and MBM-acidified significantly increased the inorganic resin-P and $NaHCO_3$-P pools in both distances analysed compared to the negative control. These pools are considered the labile P (Sharpley et al. 1984) and can be correlated with plant available-P (Schoenau and Huang 1991), indicating that the acidification of MBM and DSF can increase not only the P solubility of these biowastes but also their P fertiliser value when placed in the soil. Indeed, the soil used in this study has a low sorption capacity (Sica, Kopp, Müller-Stöver, et al. 2023), which explains the high P contents in these more labile pools. However, these values were less for both acidified biowastes than for the TSP in both distances, probably due to the co-application and release of other elements to the soil and changes in the pH (Sica, Kopp, Müller-Stöver, et al. 2023), which increase the P precipitation in the placement zone and surrounding soil (Meyer et al. 2021).

The localised application of mineral and organic P fertilisers creates a nutrient-rich zone in the placement zone and its surrounding soil, and the P interaction with other elements and the soil chemical properties has a strong influence on the P speciation (Meyer et al. 2020). In this study, both acidified biowastes and the TSP had significant increases in the inorganic NaOH-P fractions compared to the negative control. This is in agreement

13652389, 2025, 2, Downloaded from https://bsssjournals.onlinelibrary.wiley.com/doi/10.1111/ejss.70076 by Capes, Wiley Online Library on [17/03/2025]. See the Terms and Conditions (https://onlinelibrary.wiley.com/terms-and-conditions) on Wiley Online Library for rules of use; OA articles are governed by the applicable Creative Commons License

with Meyer et al. (2021), who found that in non-calcareous soils (the case of the one used in this study), precipitation of aluminium-P regulates P availability.

Although the accuracy and interpretation of the Hedley fractions still generate debates in the literature (Barrow et al. 2020; Gu and Margenot 2020; Barrow and Debnath 2020), the NaOH-P fraction may extract Fe- and Al-bond P (Wang et al. 2013), which would confirm the tendency of soils from the CRUCIAL field experiment to precipitate Fe- and Al-P. In addition to that, the formation of more stable Ca-P species as hydroxyapatite in soils would require longer incubation times (Meyer et al. 2021, 2023) and is favoured by pH above 8 (Wang et al. 2010), which was not reached during our experiment. It is worth noting that the sum of the P recovered in the Hedley and microbial P pools was relatively lower than the amount of P released to the soil for the TSP and MBM-acidified. This could be because this methodology may not be accurate in quantifying different P fractions and can under-estimate them (Barrow et al. 2020; Guppy 2021).

4.3 | P Release and Movement in the Soil

Phosphorus diffusion in the soil solution is a physical process that can be substantially affected by chemical processes (Meyer et al. 2023), soil type, including its sorption capacity (Degryse and McLaughlin 2014; Meyer et al. 2020, 2023), and biotic processes (Olander and Vitousek 2004). In our study, the TSP and the increased P solubility of MBM and DSF due to the acidification clearly increased the P diffusion rates in the soil (Figure 4). For the TSP, the resin-P contents were considerably large even at 10–12 mm from the placement zone after 12 days of incubation. These values are in agreement with Hao et al. (2002) and Rech et al. (2018), who found that after 14 days, the P from mineral fertilisers diffused up to 17 and 20 mm, respectively. Thus, this indicates that for the TSP the P diffused to further distances than we analysed in this study. These high diffusion rates are likely due to the low P sorption capacity of the soil used in this study (Eghball et al. 1990; Meyer et al. 2023).

The DSF-acidified also had a relatively large resin-P content at 10–12 mm. Interestingly, DSF-acidified was the only fertiliser that did not show a significant difference in resin-P between distances. Consequently, the resin-P concentration at different distances for DSF-acidified did not fit the three-parameter exponential decay equation; instead, it resembled a flat line parallel to the x-axis. We speculate that the low soil pH could have increased P precipitation, as at pH between 3 and 5 the P fixation by Al and Fe is favoured (Price 2006; Penn and Camberato 2019).

For both untreated biowastes, the P diffusion rate was considerably less and mainly restricted to the first 8 mm from the placement zone. As demonstrated by Sica, Kopp, Müller-Stöver, et al. (2023), the P released from the fertiliser to the soil is highly correlated with the fertiliser P solubility, which is low for the untreated DSF and MBM, compared to their acidified counterparts. In addition to that, the diffusion rate in the soils is driven by the concentration gradient of labile-P between the source (fertiliser) and the soil (Degryse and McLaughlin 2014; Degryse et al. 2017), which explains the effects of acidification on increasing the P diffusion in the soil.

The measurements of microbial-P at various distances from the placement zone exhibited relatively high errors. While potential differences between distances were observed for fertilisers such as DSF-acidified and MBM-acidified, significant differences were found only for MBM-untreated. The data also revealed that the curve fitted the three-parameter exponential decay model for MBM-untreated. Specifically, for MBM-untreated, microbial-P levels remained relatively high up to 8 mm from the fertiliser layer, suggesting that P is being transported from the fertiliser placement zone through the soil due to microbial growth. This phenomenon may be attributed to the substantial release of C and N into the soil by MBM-untreated, which is subsequently incorporated by the microbial biomass, thus stimulating microbial activity and growth, as previously discussed and demonstrated in Figure 6.

In soils with low P availability, as the one used in this study, microbial immobilisation is the main P flux, with the labile P being rapidly biologically cycled (Pistocchi et al. 2018). Thus, it is likely that the C and N provided by the MBM-untreated and the low C/N ratio in the placement zone stimulated microbial growth, and the microorganisms incorporated the P from the MBM-untreated placement zone to sustain the high growth rates, transporting it through the soil disc, explaining the high microbial P content at different soil layers.

4.4 | δ^{18}O-P

In this study, the incubation was conducted at 15°C, and we initiated the experiment by introducing ^{18}O-enriched water. According to Equation (1) (Chang and Blake 2015), we expected the soil δ^{18}O-P to be +13.6‰ before incubation and +30.9‰ after 12 days of incubation with the enriched water. This was based on the hypothesis of biological cycling of P and of the deriving isotopic equilibrium of oxygen between water and phosphate promoted by pyrophosphatase. However, in none of the treatments were resin nor microbial δ^{18}O-P close to the calculated equilibrium value.

The pyrophosphatase is a reversible, fast and ubiquitous enzyme that can hydrolyze pyrophosphate ($P_2O_7^{-4}$) and incorporates an oxygen atom from the surrounding water. Its continuous action of pyrophosphatase brings oxygen in phosphates into isotopic equilibrium between surrounding water. Also, as shown in Cohn (1958), oxygen exchange with water can occur at the mere docking of phosphate into the enzyme. The equilibrium of the phosphate δ^{18}O and soil water can be reached within a scale of hours or just a few days under controlled conditions with sterilised and less complex substrate, with labile C, as demonstrated by Chang and Blake (2015) and von Sperber et al. (2017). It is further assumed that whenever biological activity is present, oxygen in phosphate readily reaches equilibrium with water because pyrophosphate is ubiquitously present in all cells. However, in complex media, particularly in soils, deviations from the oxygen isotope equilibrium are often observed (von Sperber et al. 2023). In incubation studies with soils, (Gross and Angert 2015) found that the resin δ^{18}O-P values reached the expected equilibrium values within less than 14 days. Indeed, Pistocchi et al. (2020) observed that the resin δ^{18}O-P values reached the expected equilibrium with soil water in a soil with high P availability within a few days. However, for a soil

13652389, 2025, 2, Downloaded from https://bsssjournals.onlinelibrary.wiley.com/doi/10.1111/ejss.70076 by Capes, Wiley Online Library on [17/03/2025]. See the Terms and Conditions (https://onlinelibrary.wiley.com/terms-and-conditions) on Wiley Online Library for rules of use; OA articles are governed by the applicable Creative Commons License

with low available P, the resin δ^{18}O-P did not reach the expected equilibrium even after 93 days of incubation.

In this study, the soil had low P availability and a low degree of P saturation (24%), according to Lemming et al. (2019). Thus, the soluble P applied can be sorbed onto the soil surfaces, preventing it from being exchanged with the soil solution and, therefore, being microbially processed (Sinaj et al. 1997). Therefore, according to Pistocchi et al. (2020), longer incubation periods may be required for the resin-P δ^{18}O to reach the theoretical equilibrium of oxygen in phosphate with soil water in soils with low available P.

In a 34-day incubation involving four different soils, Siegenthaler et al. (2020) found an increase in microbial and resin-P δ^{18}O values. However, they did not reach the expected soil-water equilibrium. According to them, their findings indicate that ^{18}O from the water was incorporated into the microbial-P, but the complete turnover of microbial-P did not occur even after 34 days. Thus, Siegenthaler et al. (2020) suggested that in heterogeneous and complex environments like soils, which host a diversity of active microorganisms (Tiedje et al. 1999), isotopic equilibration of oxygen between phosphate and water, as promoted by pyrophosphatase, can be slower and may require extended periods to be attained. In our study, the incubation period was even shorter, just 12 days. The untreated MBM was the treatment with the highest respiration at 12 days and had the highest contribution of $\delta^{18}OEq_{watersoil}$ to the microbial-P δ^{18}O values. However, when considering the source contribution to the resin-P δ^{18}O values, for all treatments in this study, $\delta^{18}OEq_{watersoil}$ had little or negligible contribution.

Our results, particularly for MBM-untreated, indicate that this duration was adequate for microorganisms to thrive and assimilate and biologically cycle P into the microbial biomass, as the microbial activity, expressed by respired CO_2, was significant and positively correlated with the ^{18}O incorporation into the microbial-P (Figure 3). Other incubation studies employing enriched ^{18}O water have consistently shown a positive correlation between microbial respiration and the incorporation of oxygen from the water into microbial P (Melby et al. 2013; Siegenthaler et al. 2020). Our findings align with this pattern, as MBM-untreated exhibited the highest cumulative respiration, microbial-P content in the soil, and a statistically significant increase in microbial-P δ^{18}O at both distances, in comparison to the negative control. In contrast, the MBM-acidified also had a relatively high respiration and C and N release to the soil, but we did not observe significant changes in the microbial-P δ^{18}O values nor in the soil microbial-P concentrations.

However, during this period, the equilibrated phosphate was not released to the soil solution. Thus, the soil solution did not reach the equilibrium values. This is confirmed by two of our findings. First, after 12 days, for all treatments, the main sources contributing to the resin-P δ^{18}O values were the fertiliser and the initial soil resin-P. In the case of DSF-acidified, it was mainly the HCl-pool (Table S3). Second, ^{18}O incorporation into the resin-P did not have a significant correlation with microbial respiration, being masked by the phosphates released abiotically from the fertiliser, mainly the TSP (Figure 3). The low nutrient concentration in the soil used in this study inherently restricts microbial growth (Muñoz et al. 2017; Gómez-Muñoz et al. 2018). Consequently, MBM-untreated provided a substantial amount of C, N, and P, enabling robust microbial growth and P assimilation. Nevertheless, we suggest that over a more extended incubation period, microorganisms would undergo turnover of these elements, potentially led by limitations in other nutrients, such as C and N and release P into the soil. This release would change the resin-P δ^{18}O values, eventually approaching the expected equilibrium with soil water.

In this study, we observed the highest resin-P δ^{18}O values for triple superphosphate (TSP) at 0–2 and 4–6 mm from the placement zone. Interestingly, these values in the soil were approximately +21‰, almost the same values as the initial δ^{18}O-P values of the fertiliser. Gross et al. (2015) similarly reported the preservation of TSP resin-P δ^{18}O values in the soil, even after 8 weeks of incubation. They suggested that the large quantity of soluble P introduced into the soil along with the fertiliser might have masked microbial P turnover due to the low microbial activity in the soil.

In contrast, for the DSF-acidified treatment, despite observing a high release of P to the soil and an increase in soil resin-P content, the resin-P δ^{18}O values in the soil at both distances were lower than those of the fertiliser (+15.7‰), the soil resin-P at T0 (+14.6‰), and the theoretical equilibrium (+30.9‰), which made it not possible to run the proposed model with three sources on IsoSource. The HCl-P pool of the soil used in this study was previously determined as +10.8‰. Thus, for the DSF-acidified treatment, we suggest that the HCl-P pool may have been a fourth source (Table S4), as the significant reduction in soil pH, reaching around 4 at both distances, could have contributed to the release of P from the HCl-P pool (Wu et al. 2014).

However, the HCl-P pool concentration did not show a significant change compared to the negative control. Instead, pH variations may have increased the exchangeability between this pool and the P released from the fertiliser to the soil (Turner and Blackwell 2013). Therefore, even with the high amounts of P released from the fertiliser to the soil and a significant increase in soil resin-P, the DSF-acidified resin-P δ^{18}O values were not imprinted in the soil resin-P δ^{18}O values, indicating that the placement of DSF-acidified intensified abiotic processes compared to the placement of TSP, probably due to the strong effect on soil pH and the release of other elements.

4.5 | Practical Application and Future Research

Replacing mineral P fertilisers is one approach to making agriculture more sustainable, reducing dependence on external resources, and ensuring food security in importing countries (Salas et al. 2024). However, according to Moshkin et al. (2023), farmers are willing to pay 30%–46% less per unit of P from biowaste compared to mineral fertilisers. This is mainly due to the lower and uncertain P availability and content of these materials (Tur-Cardona et al. 2018). Therefore, increasing the P availability of biowastes would also increase the interest of farmers and their potential to replace mineral P fertilisers. Our results show that acidification can significantly increase the P solubility of biowastes, their release to the soil and, consequently, the resin P

13652389, 2025, 2, Downloaded from https://bsssjournals.onlinelibrary.wiley.com/doi/10.1111/ejss.70076 by Capes, Wiley Online Library on [17/03/2025]. See the Terms and Conditions (https://onlinelibrary.wiley.com/terms-and-conditions) on Wiley Online Library for rules of use; OA articles are governed by the applicable Creative Commons License

in the soil, which is highly correlated with the plant available P (Mallarino and Atia 2005).

These results are in agreement with Sica, Kopp, Magid, et al. (2023) and Sica and Magid (2024) who found that the placement of acidified DSF and MBM significantly increased P uptake by 10 different crops compared to their respective untreated materials. The authors also point out that the increased P availability would allow farmers to apply lower amounts of P, especially in phosphorus-saturated soils. Thus, acidified biowaste could be used as a starter fertiliser (Regueiro et al. 2020), reducing the accumulation of P in soils around animal production areas and reducing the risk of leaching and runoff and, consequently, eutrophication (Fischer et al. 2017).

It is important to note that this study focused on understanding the short-term biotic and abiotic processes influencing phosphorus dynamics in soil, with acidified biowastes used as starter fertilisers. The emphasis was on a short-term agronomic perspective. Consequently, further research is required to evaluate how acidification impacts additional factors related to soil health and microbial community and function, both in the short and long term, to fully understand its broader implications for sustainable soil management.

5 | Conclusions

In conclusion, our results indicate that the placement of different fertilisers intensifies biogeochemical processes in the placement zone and surrounding soil. These processes were highly affected by the fertiliser composition and acidification (Hypothesis 1: *Fertiliser composition and acidification pre-treatment will affect biotic and abiotic processes in the placement zone and surrounding soil*).

After 12 days of incubation, our results demonstrate a significant correlation between microbial respiration and ^{18}O incorporation in microbial-P. Untreated meat and bone meal produced the highest respiration rates, and it was the only treatment with significant differences in microbial-P contents at different soil distances. Thus, these results indicate that for this fertiliser, the co-occurrence of diffusion and biotic processes such as microbial growth could be the main P transport mechanisms through the soil (Hypothesis 2: *For untreated biowastes, P movement from the placement zone through the soil is primarily driven by biotic processes* (*as indicated by intracellular isotopic equilibration of oxygen between water and phosphate and by released of phosphate by hydrolytic enzymes*), *with microbial growth serving as the principal transport mechanism*).

Acidification significantly reduced microbial respiration by 82% and 29%, inhibiting microbial growth in the treatments with DSF and MBM, respectively. Acidification also significantly increased the amount of P released (DSF: from 6.2% to 69% and for MBM: from 11% to 51% of the total P applied) from the fertiliser to the soil, as well as soil resin-P contents, indicating that for acidified biowastes (and triple superphosphate), the movement of P from the placement zone through the soil was primarily driven by abiotic processes, with diffusion as the main transport mechanism (Hypothesis 3: *The placement of acidified biowastes will increase the soluble P applied and lower the soil pH surrounding the placement zone to levels that inhibit microbial activity. As a result, the movement of P from the placement zone through the soil will be primarily driven by abiotic processes, with diffusion as the main transport mechanism*).

The observed effects on biogeochemical processes and nutrient dynamics highlight significant implications for agricultural practices and sustainable soil management. The study reveals that the placement of different fertilisers, particularly acidified biowastes, can profoundly influence both biotic and abiotic processes in the soil. Untreated meat and bone meal, which exhibited high microbial respiration and significant biotic activity, suggests that microbial growth can be a crucial driver of P transport through the soil. In contrast, acidification significantly reduces microbial respiration, indicating a shift towards abiotic processes like diffusion for P movement. This underscores the potential of acidified biowastes to enhance P availability and recycling efficiency in agriculture. Integrating these findings into soil management strategies could improve fertiliser efficiency, optimise nutrient use, and promote sustainable agricultural practices by balancing biotic and abiotic mechanisms to maximise nutrient availability and reduce dependency on synthetic fertilisers.

Author Contributions

Pietro Sica: conceptualization, methodology, software, data curation, formal analysis, validation, investigation, visualization, project administration, writing – original draft, writing – review and editing. **Maria Monrad Rieckmann:** conceptualization, methodology, investigation, writing – original draft. **Mario Álvarez Salas:** conceptualization, methodology, investigation, formal analysis, visualization, writing – review and editing, writing – original draft. **Jakob Magid:** conceptualization, data curation, investigation, formal analysis, funding acquisition, project administration, supervision, resources. **Federica Tamburini:** resources, project administration, visualization, funding acquisition, writing – original draft, writing – review and editing, methodology, conceptualization, data curation, supervision, formal analysis, validation, investigation, software.

Acknowledgements

This project has received funding from the European Union's Horizon 2020 research and innovation programme under the Marie Sklodowska-Curie grant agreement No. 860127 and from the Independent Research Fund Denmark, under the project PROCESSOR (Phosphorus Recycling frOm Complex scarcEly Soluble Societal resources – letting the sOil do the work), grant number 1032-00011B.

Conflicts of Interest

The authors declare no conflicts of interest.

Data Availability Statement

All data is openly available online in ERDA, the repository of the University of Copenhagen at the following link: https://doi.org/10.17894/ucph.4501269f-c992-477c-be52-331de9b99c5b.

References

Al Seadi, T., B. Drosg, W. Fuchs, et al. 2013. "Biogas Digestate Quality and Utilization." In *The Biogas Handbook*, 267–301. Elsevier.

13652389, 2025, 2, Downloaded from https://bsssjournals.onlinelibrary.wiley.com/doi/10.1111/ejss.70076 by Capes, Wiley Online Library on [17/03/2025]. See the Terms and Conditions (https://onlinelibrary.wiley.com/terms-and-conditions) on Wiley Online Library for rules of use; OA articles are governed by the applicable Creative Commons License

Alef, K. 1995. "Soil Respiration." In *Methods in Applied Soil Microbiology and Biochemistry*, edited by K. Alef and P. Nannipieri, 214–219. Academic Press Inc.

Baffes, J., and W. C. Koh. 2022. *Fertilizer Prices Expected To Remain Higher For Longer*. World Bank.

Baral, K. R., I. F. Pedersen, G. H. Rubæk, and P. Sørensen. 2021. "Placement Depth and Distribution of Cattle Slurry Influence Initial Maize Growth and Phosphorus and Nitrogen Uptake." *Journal of Plant Nutrition and Soil Science* 184: 461–470. https://doi.org/10.1002/jpln.202000492.

Barrow, N. J., and A. Debnath. 2020. "Reply to: Navigating Limitations and Opportunities of Soil Phosphorus Fractionation: A Comment on 'the Soil Phosphate Fractionation Fallacy' by Barrow et al. 2020." *Plant and Soil* 453: 595–596.

Barrow, N. J., A. Sen, N. Roy, and A. Debnath. 2020. "The Soil Phosphate Fractionation Fallacy." *Plant and Soil* 459, no. 1-2: 1–11. https://doi.org/10.1007/s11104-020-04476-6.

Blake, R. E., J. R. O'Neil, and A. V. Surkov. 2005. "Biogeochemical Cycling of Phosphorus: Insights From Oxygen Isotope Effects of Phosphoenzymes." *American Journal of Science* 305: 596–620. https://doi.org/10.2475/ajs.305.6-8.596.

Brod, E., A. F. Øgaard, E. Hansen, et al. 2015. "Waste Products as Alternative Phosphorus Fertilisers Part I: Inorganic P Species Affect Fertilisation Effects Depending on Soil pH." *Nutrient Cycling in Agroecosystems* 103: 167–185. https://doi.org/10.1007/S10705-015-9734-1/FIGURES/3.

Brod, E., A. F. Øgaard, T. K. Haraldsen, and T. Krogstad. 2015. "Waste Products as Alternative Phosphorus Fertilisers Part II: Predicting P Fertilisation Effects by Chemical Extraction." *Nutrient Cycling in Agroecosystems* 103: 187–199. https://doi.org/10.1007/S10705-015-9731-4/FIGURES/2.

Bruun, S., S. L. Harmer, G. Bekiaris, et al. 2017. "The Effect of Different Pyrolysis Temperatures on the Speciation and Availability in Soil of P in Biochar Produced From the Solid Fraction of Manure." *Chemosphere* 169: 377–386. https://doi.org/10.1016/j.chemosphere.2016.11.058.

Bünemann, E. K., S. Augstburger, and E. Frossard. 2016. "Dominance of Either Physicochemical or Biological Phosphorus Cycling Processes in Temperate Forest Soils of Contrasting Phosphate Availability." *Soil Biology and Biochemistry* 101: 85–95. https://doi.org/10.1016/j.soilbio.2016.07.005.

Chang, S. J., and R. E. Blake. 2015. "Precise Calibration of Equilibrium Oxygen Isotope Fractionations Between Dissolved Phosphate and Water From 3 to 37°C." *Geochimica et Cosmochimica Acta* 150: 314–329. https://doi.org/10.1016/j.gca.2014.10.030.

Chaves, C., R. Canet, R. Albiach, et al. 2006. "Meat and Bone Meal: Fertilizing Value and Rates of Nitrogen Mineralization." *Nutrient and Carbon Cycling in Sustainable Plant-Soil Systems* 1: 1–4.

Christiansen, N. H., P. Sørensen, R. Labouriau, B. T. Christensen, and G. H. Rubæk. 2020. "Characterizing Phosphorus Availability in Waste Products by Chemical Extractions and Plant Uptake." *Journal of Plant Nutrition and Soil Science* 183: 416–428.

Chuda, A., K. Ziemin'ski, and Z. Ziemin'ski. 2021. "Digestate Mechanical Separation in Industrial Conditions: Efficiency Profiles and Fertilising Potential." *Waste Management* 128: 106–116. https://doi.org/10.1016/j.wasman.2021.04.049.

Cohn, M. 1958. "Phosphate-Water Exchange Reaction Catalyzed by Inorganic Pyrophosphatase of Yeast." *Journal of Biological Chemistry* 230: 369–379. https://doi.org/10.1016/S0021-9258(18)70572-3.

Degryse, F., R. Baird, R. C. da Silva, and M. J. McLaughlin. 2017. "Dissolution Rate and Agronomic Effectiveness of Struvite Fertilizers—Effect of Soil pH, Granulation and Base Excess." *Plant and Soil* 410: 139–152. https://doi.org/10.1007/s11104-016-2990-2.

Degryse, F., and M. J. McLaughlin. 2014. "Phosphorus Diffusion From Fertilizer: Visualization, Chemical Measurements, and Modeling." *Soil Science Society of America Journal* 78: 832–842. https://doi.org/10.2136/sssaj2013.07.0293.

van Dijk, K. C., J. P. Lesschen, and O. Oenema. 2016. "Phosphorus Flows and Balances of the European Union Member States." *Science of the Total Environment* 542: 1078–1093. https://doi.org/10.1016/j.scitotenv.2015.08.048.

Ebina, J., T. Tsutsui, and T. Shirai. 1983. "Simultaneous Determination of Total Nitrogen and Total Phosphorus in Water Using Peroxodisulfate Oxidation." *Water Research* 17: 1721–1726. https://doi.org/10.1016/0043-1354(83)90192-6.

Eghball, B., D. H. Sander, and J. Skopp. 1990. "Diffusion, Adsorption, and Predicted Longevity of Banded Phosphorus Fertilizer in Three Soils." *Soil Science Society of America Journal* 54: 1161–1165. https://doi.org/10.2136/sssaj1990.03615995005400040041x.

Fischer, P., R. Pöthig, and M. Venohr. 2017. "The Degree of Phosphorus Saturation of Agricultural Soils in Germany: Current and Future Risk of Diffuse P Loss and Implications for Soil P Management in Europe." *Science of the Total Environment* 599–600: 1130–1139. https://doi.org/10.1016/j.scitotenv.2017.03.143.

Frossard, E., D. L. Achat, S. M. Bernasconi, et al. 2011. "The Use of Tracers to Investigate Phosphate Cycling in Soil–Plant Systems." In *Phosphorus in Action. Soil Biology*, edited by E. Bünemann, A. Oberson, and E. Frossard, vol. 26, 59–91. Springer. https://doi.org/10.1007/978-3-642-15271-9_3.

Girkin, N. T., and H. V. Cooper. 2022. *Nitrogen and Ammonia in Soils*. 2nd ed. Elsevier Ltd.

Gómez-Muñoz, B., L. S. Jensen, A. de Neergaard, et al. 2018. "Effects of Penicillium Bilaii on Maize Growth Are Mediated by Available Phosphorus." *Plant and Soil* 431: 159–173. https://doi.org/10.1007/S11104-018-3756-9.

Gross, A., and A. Angert. 2015. "What Processes Control the Oxygen Isotopes of Soil Bio-Available Phosphate?" *Geochimica et Cosmochimica Acta* 159: 100–111. https://doi.org/10.1016/j.gca.2015.03.023.

Gross, A., B. L. Turner, S. J. Wright, et al. 2015. "Oxygen Isotope Ratios of Plant Available Phosphate in Lowland Tropical Forest Soils." *Soil Biology and Biochemistry* 88: 354–361. https://doi.org/10.1016/j.soilbio.2015.06.015.

Gu, C., and A. J. Margenot. 2020. "Navigating Limitations and Opportunities of Soil Phosphorus Fractionation." *Plant and Soil* 459: 13–17.

Guppy, C. 2021. "Is Soil Phosphorus Fractionation as Valuable as We Think?" *Plant and Soil* 459: 19–21. https://doi.org/10.1007/s11104-020-04817-5.

Hao, X., C. M. Cho, G. J. Racz, and C. Chang. 2002. "Chemical Retardation of Phosphate Diffusion in an Acid Soil as Affected by Liming." *Nutrient Cycling in Agroecosystems* 64: 213–224.

Hedley, M. J., J. W. B. Stewart, and B. S. Chauhan. 1982. "Changes in Inorganic and Organic Soil Phosphorus Fractions Induced by Cultivation Practices and by Laboratory Incubations." *Soil Science Society of America Journal* 46: 970–976. https://doi.org/10.2136/sssaj1982.03615995004600050017x.

Hernandez-Mora, A., O. Duboc, E. Lombi, et al. 2024. "Fertilization Efficiency of Thirty Marketed and Experimental Recycled Phosphorus Fertilizers." *Journal of Cleaner Production* 467: 142957. https://doi.org/10.1016/j.jclepro.2024.142957.

Ibendahl, G. 2022. *The Russia-Ukraine Conflict and the Effect on Fertilizer*. Kansas State University. https://agmanager.info/sites/default/files/pdf/Ibendah_Fertizer_RussiaUkraine_03-08-22.pdf.

Jeng, A., T. K. Haraldsen, N. Vagstad, et al. 2004. "Meat and Bone Meal as Nitrogen Fertilizer to Cereals in Norway." *Agricultural and Food Science* 13: 268–275. https://doi.org/10.2137/1239099042643080.

13652389, 2025, 2, Downloaded from https://bsssjournals.onlinelibrary.wiley.com/doi/10.1111/ejss.70076 by Capes, Wiley Online Library on [17/03/2025]. See the Terms and Conditions (https://onlinelibrary.wiley.com/terms-and-conditions) on Wiley Online Library for rules of use; OA articles are governed by the applicable Creative Commons License

Jeng, A. S., T. K. Haraldsen, A. Grønlund, and P. A. Pedersen. 2007. "Meat and Bone Meal as Nitrogen and Phosphorus Fertilizer to Cereals and Rye Grass." In *Advances in Integrated Soil Fertility Management in Sub-Saharan Africa: Challenges and Opportunities*, edited by A. Bationo, B. Waswa, J. Kihara, and J. Kimetu, 245–253. Springer.

Kivelä, J., L. Chen, S. Muurinen, P. Kivijärvi, V. Hintikainen, and J. Helenius. 2015. "Effects of Meat Bone Meal as Fertilizer on Yield and Quality of Sugar Beet and Carrot." *Agricultural and Food Science* 24: 68–83. https://doi.org/10.23986/AFSCI.8587.

Kopp, C., P. Sica, C. Lu, et al. 2023. "Increasing Phosphorus Plant Availability From P-Rich Ashes and Biochars by Acidification With Sulfuric Acid." *Journal of Environmental Chemical Engineering* 11, no. 6: 111489. https://doi.org/10.1016/j.jece.2023.111489.

Lemming, C., A. Oberson, J. Magid, et al. 2019. "Residual Phosphorus Availability After Long-Term Soil Application of Organic Waste." *Agriculture, Ecosystems and Environment* 270: 65–75. https://doi.org/10.1016/j.agee.2018.10.009.

Liang, Y., and R. E. Blake. 2006. "Oxygen Isotope Composition of Phosphate in Organic Compounds: Isotope Effects of Extraction Methods." *Organic Geochemistry* 37: 1263–1277. https://doi.org/10.1016/j.orggeochem.2006.03.009.

Liu, J., A. de Neergaard, and L. S. Jensen. 2019. "Increased Retention of Available Nitrogen During Thermal Drying of Solids of Digested Sewage Sludge and Manure by Acid and Zeolite Addition." *Waste Management* 100: 306–317. https://doi.org/10.1016/J.WASMAN.2019.09.019.

López-Rayo, S., K. H. Laursen, J. D. S. Lekfeldt, F. Delle Grazie, and J. Magid. 2016. "Long-Term Amendment of Urban and Animal Wastes Equivalent to More Than 100 Years of Application Had Minimal Effect on Plant Uptake of Potentially Toxic Elements." *Agriculture, Ecosystems and Environment* 231: 44–53. https://doi.org/10.1016/J.AGEE.2016.06.019.

Mallarino, A. P., and A. M. Atia. 2005. "Correlation of a Resin Membrane Soil Phosphorus Test With Corn Yield and Routine Soil Tests." *Soil Science Society of America Journal* 69: 266. https://doi.org/10.2136/sssaj2005.0266.

Melby, E. S., D. J. Soldat, and P. Barak. 2013. "Biological Decay of 18O-Labeled Phosphate in Soils." *Soil Biology and Biochemistry* 63: 124–128. https://doi.org/10.1016/j.soilbio.2013.03.020.

Meyer, G., M. J. Bell, C. L. Doolette, et al. 2020. "Plant-Available Phosphorus in Highly Concentrated Fertilizer Bands: Effects of Soil Type, Phosphorus Form, and Coapplied Potassium." *Journal of Agricultural and Food Chemistry* 68: 7571–7580. https://doi.org/10.1021/acs.jafc.0c01287.

Meyer, G., M. J. Bell, P. M. Kopittke, et al. 2023. "Mobility and Lability of Phosphorus From Highly Concentrated Fertiliser Bands." *Geoderma* 429: 116248. https://doi.org/10.1016/J.GEODERMA.2022.116248.

Meyer, G., M. J. Bell, E. Lombi, et al. 2021. "Phosphorus Speciation in the Fertosphere of Highly Concentrated Fertilizer Bands." *Geoderma* 403: 115208. https://doi.org/10.1016/J.GEODERMA.2021.115208.

Möller, K., and T. Müller. 2012. "Effects of Anaerobic Digestion on Digestate Nutrient Availability and Crop Growth: A Review." *Engineering in Life Sciences* 12: 242–257. https://doi.org/10.1002/ELSC.201100085.

Moshkin, E., S. Garmendia Lemus, L. Bamelis, and J. Buysse. 2023. "Assessment of Willingness-To-Pay for Bio-Based Fertilisers Among Farmers and Agricultural Advisors in the EU." *Journal of Cleaner Production* 414: 137548. https://doi.org/10.1016/j.jclepro.2023.137548.

Gómez-Muñoz, B., J. Magid, and L. S. Jensen. 2017. "Nitrogen Turnover, Crop Use Efficiency and Soil Fertility in a Long-Term Field Experiment Amended With Different Qualities of Urban and Agricultural Waste." *Agriculture, Ecosystems and Environment* 240: 300–313. https://doi.org/10.1016/J.AGEE.2017.01.030.

Nkebiwe, P. M., G. Neumann, and T. Müller. 2017. "Densely Rooted Rhizosphere Hotspots Induced Around Subsurface NH4+-Fertilizer Depots: A Home for Soil PGPMs?" *Chemical and Biological Technologies in Agriculture* 4: 1–16. https://doi.org/10.1186/S40538-017-0111-Y/TABLES/2.

NSW. 1995. *Soil Survey Standard Test Method—Phosphorus Sorption*. New South Wales Department of Sustainable Natural Resources.

Oehl, F., E. Frossard, A. Fliessbach, D. Dubois, and A. Oberson. 2004. "Basal Organic Phosphorus Mineralization in Soils Under Different Farming Systems." *Soil Biology and Biochemistry* 36: 667–675. https://doi.org/10.1016/J.SOILBIO.2003.12.010.

Olander, L. P., and P. M. Vitousek. 2004. "Biological and Geochemical Sinks for Phosphorus in Soil From a Wet Tropical Forest." *Ecosystems* 7: 404–419. https://doi.org/10.1007/s10021-004-0264-y.

Pan, W. L., I. J. Madsen, R. P. Bolton, L. Graves, and T. Sistrunk. 2016. "Ammonia/Ammonium Toxicity Root Symptoms Induced by Inorganic and Organic Fertilizers and Placement." *Agronomy Journal* 108: 2485–2492. https://doi.org/10.2134/AGRONJ2016.02.0122.

Panuccio, M. R., F. Romeo, C. Mallamaci, and A. Muscolo. 2021. "Digestate Application on Two Different Soils: Agricultural Benefit and Risk." *Waste and Biomass Valorization* 12: 4341–4353. https://doi.org/10.1007/s12649-020-01318-5.

Pedersen, I. F., P. Sørensen, K. R. Baral, and G. H. Rubæk. 2020. "Damage to the Primary Root in Response to Cattle Slurry Placed Near Seed May Compromise Early Growth of Corn." *Agronomy Journal* 112: 1346–1359. https://doi.org/10.1002/agj2.20097.

Penn, C. J., and J. J. Camberato. 2019. "A Critical Review on Soil Chemical Processes That Control How Soil Ph Affects Phosphorus Availability to Plants." *Agriculture* 9, no. 6: 1–18. https://doi.org/10.3390/AGRICULTURE9060120.

Pistocchi, C., É. Mészáros, E. Frossard, E. K. Bünemann, and F. Tamburini. 2020. "In or out of Equilibrium? How Microbial Activity Controls the Oxygen Isotopic Composition of Phosphate in Forest Organic Horizons With Low and High Phosphorus Availability." *Frontiers in Environmental Science* 8: 1–15. https://doi.org/10.3389/fenvs.2020.564778.

Pistocchi, C., É. Mészáros, F. Tamburini, E. Frossard, and E. K. Bünemann. 2018. "Biological Processes Dominate Phosphorus Dynamics Under Low Phosphorus Availability in Organic Horizons of Temperate Forest Soils." *Soil Biology and Biochemistry* 126: 64–75. https://doi.org/10.1016/j.soilbio.2018.08.013.

Price, G. 2006. *Australian Soil Fertility Manual*. 1st ed. CSIRO.

Recena, R., A. M. García-López, J. M. Quintero, et al. 2022. "Assessing the Phosphorus Demand in European Agricultural Soils Based on the Olsen Method." *Journal of Cleaner Production* 379: 1–12. https://doi.org/10.1016/j.jclepro.2022.134749.

Rech, I., P. J. A. Withers, D. L. Jones, and P. S. Pavinato. 2018. "Solubility, Diffusion and Crop Uptake of Phosphorus in Three Different Struvites." *Sustainability* 11, no. 1: 134. https://doi.org/10.3390/SU11010134.

Regueiro, I., P. Siebert, J. Liu, D. Müller-Stöver, and L. S. Jensen. 2020. "Acidified Animal Manure Products Combined With a Nitrification Inhibitor Can Serve as a Starter Fertilizer for Maize." *Agronomy* 10: 1941. https://doi.org/10.3390/agronomy10121941.

Rieckmann, M. M., R. E. Blake, S. J. Chang, and K. H. Laursen. 2024. "An Optimized Method for Extraction and Purification of Inorganic Phosphate From Plant Material for Oxygen Isotope Ratio Analysis." *MethodsX* 12: 102541. https://doi.org/10.1016/j.mex.2023.102541.

Ruess, L., and H. Ferris. 2004. "Decomposition Pathways and Successional Changes." In *Fourth International Congress of Nematology*, 547–556. Brill.

Salas, M. A., P. Sica, T. J. Sitzmann, et al. 2024. "Current Challenges on the Widespread Adoption of New Bio-Based Fertilizers: Insights to Move Forward Towards More Circular Food Systems." *Frontiers in*

13652389, 2025, 2, Downloaded from https://bsssjournals.onlinelibrary.wiley.com/doi/10.1111/ejss.70076 by Capes, Wiley Online Library on [17/03/2025]. See the Terms and Conditions (https://onlinelibrary.wiley.com/terms-and-conditions) on Wiley Online Library for rules of use; OA articles are governed by the applicable Creative Commons License

Sustainable Food Systems 8: 1–19. https://doi.org/10.3389/fsufs.2024.1386680.

Schoenau, J. J., and W. Z. Huang. 1991. "Anion-Exchange Membrane, Water, and Sodium Bicarbonate Extractions as Soil Tests for Phosphorus." *Communications in Soil Science and Plant Analysis* 22: 465–492. https://doi.org/10.1080/00103629109368432.

Sharpley, A. N., C. A. Jones, C. Gray, and C. V. Cole. 1984. "A Simplified Soil and Plant Phosphorus Model: II. Prediction of Labile, Organic, and Sorbed Phosphorus." *Soil Science Society of America Journal* 48: 805–809. https://doi.org/10.2136/sssaj1984.03615995004800040021x.

Sica, P., C. Kopp, J. Magid, and D. S. Müller-Stöver. 2023. "Placement and Acidification of Biowastes: Potential Strategies for Improving Phosphorus Use Efficiency." *Environmental Technology and Innovation* 103493: 103493. https://doi.org/10.1016/j.eti.2023.103493.

Sica, P., C. Kopp, D. S. Müller-Stöver, and J. Magid. 2023. "Acidification and Alkalinization Pretreatments of Biowastes and Their Effect on P Solubility and Dynamics When Placed in Soil." *Journal of Environmental Management* 333: 117447. https://doi.org/10.1016/J.JENVMAN.2023.117447.

Sica, P., and J. Magid. 2024. "Placement of Acidified Digestate Solid Fraction as an Efficient Starter Phosphorus Fertilizer for Horticulture Crops." *Scientia Horticulturae* 328: 112961. https://doi.org/10.1016/j.scienta.2024.112961.

Siegenthaler, M. B., F. Tamburini, E. Frossard, et al. 2020. "A Dual Isotopic (32P and 18O) Incubation Study to Disentangle Mechanisms Controlling Phosphorus Cycling in Soils From a Climatic Gradient (Kohala, Hawaii)." *Soil Biology and Biochemistry* 149: 107920. https://doi.org/10.1016/j.soilbio.2020.107920.

Sinaj, S., E. Frossard, and J. C. Fardeau. 1997. "Isotopically Exchangeable Phosphate in Size Fractionated and Unfractionated Soils." *Soil Science Society of America Journal* 61: 1413–1417. https://doi.org/10.2136/sssaj1997.03615995006100050019x.

Tambone, F., P. Genevini, G. D'Imporzano, and F. Adani. 2009. "Assessing Amendment Properties of Digestate by Studying the Organic Matter Composition and the Degree of Biological Stability During the Anaerobic Digestion of the Organic Fraction of MSW." *Bioresource Technology* 100: 3140–3142. https://doi.org/10.1016/j.biortech.2009.02.012.

Tambone, F., V. Orzi, G. D'Imporzano, and F. Adani. 2017. "Solid and Liquid Fractionation of Digestate: Mass Balance, Chemical Characterization, and Agronomic and Environmental Value." *Bioresource Technology* 243: 1251–1256. https://doi.org/10.1016/j.biortech.2017.07.130.

Tamburini, F., V. Pfahler, E. K. Bünemann, K. Guelland, S. M. Bernasconi, and E. Frossard. 2012. "Oxygen Isotopes Unravel the Role of Microorganisms in Phosphate Cycling in Soils." *Environmental Science & Technology* 46: 5956–5962. https://doi.org/10.1021/es300311h.

Tiedje, J. M., S. Asuming-Brempong, K. Nüsslein, T. L. Marsh, and S. J. Flynn. 1999. "Opening the Black Box of Soil Microbial Diversity." *Applied Soil Ecology* 13: 109–122. https://doi.org/10.1016/S0929-1393(99)00026-8.

Tur-Cardona, J., O. Bonnichsen, S. Speelman, et al. 2018. "Farmers' Reasons to Accept Bio-Based Fertilizers: A Choice Experiment in Seven Different European Countries." *Journal of Cleaner Production* 197: 406–416. https://doi.org/10.1016/J.JCLEPRO.2018.06.172.

Turner, B. L., and M. S. A. Blackwell. 2013. "Isolating the Influence of pH on the Amounts and Forms of Soil Organic Phosphorus." *European Journal of Soil Science* 64: 249–259. https://doi.org/10.1111/ejss.12026.

Valsami-Jones, E., K. V. Rggnarsdottir, A. Putnis, et al. 1998. "The Dissolution of Apatite in the Presence of Aqueous Metal Cations at pH 2–7." *Chemical Geology* 151: 215–233. https://doi.org/10.1016/S0009-2541(98)00081-3.

von Sperber, C., H. Kries, F. Tamburini, S. M. Bernasconi, and E. Frossard. 2014. "The Effect of Phosphomonoesterases on the Oxygen Isotope Composition of Phosphate." *Geochimica et Cosmochimica Acta* 125: 519–527. https://doi.org/10.1016/j.gca.2013.10.010.

von Sperber, C., H. Lewandowski, F. Tamburini, S. M. Bernasconi, W. Amelung, and E. Frossard. 2017. "Kinetics of Enzyme-Catalysed Oxygen Isotope Exchange Between Phosphate and Water Revealed by Raman Spectroscopy." *Journal of Raman Spectroscopy* 48: 368–373. https://doi.org/10.1002/jrs.5053.

von Sperber, C., C. Pistocchi, M. Weiler, and F. Tamburini. 2023. "Oxygen Isotope Ratios of Phosphates in the Soil-Plant System: Limitations and Future Developments." *European Journal of Soil Science* 74: 1–14. https://doi.org/10.1111/ejss.13434.

Wang, C., Y. Zhang, H. Li, and R. J. Morrison. 2013. "Sequential Extraction Procedures for the Determination of Phosphorus Forms in Sediment." *Limnology (Tokyo)* 14: 147–157. https://doi.org/10.1007/s10201-012-0397-1.

Wang, P., C. Li, H. Gong, X. Jiang, H. Wang, and K. Li. 2010. "Effects of Synthesis Conditions on the Morphology of Hydroxyapatite Nanoparticles Produced by Wet Chemical Process." *Powder Technology* 203: 315–321. https://doi.org/10.1016/j.powtec.2010.05.023.

Wu, Y., Y. Wen, J. Zhou, and Y. Wu. 2014. "Phosphorus Release From Lake Sediments: Effects of pH, Temperature and Dissolved Oxygen." *KSCE Journal of Civil Engineering* 18: 323–329. https://doi.org/10.1007/s12205-014-0192-0.

Yan, F., S. Schubert, and K. Mengel. 1992. "Effect of Low Root Medium pH on Net Proton Release, Root Respiration, and Root Growth of Corn (*Zea Mays* L.) and Broad Bean (*Vicia Faba* L.)." *Plant Physiology* 99, no. 2: 415–421. https://doi.org/10.1104/pp.99.2.415.

Supporting Information

Additional supporting information can be found online in the Supporting Information section.

13652389, 2025, 2, Downloaded from https://bsssjournals.onlinelibrary.wiley.com/doi/10.1111/ejss.70076 by Capes, Wiley Online Library on [17/03/2025]. See the Terms and Conditions (https://onlinelibrary.wiley.com/terms-and-conditions) on Wiley Online Library for rules of use; OA articles are governed by the applicable Creative Commons License